Founded 1905

STABILIZABILITY AND DOMINANT POLE PLACEMENT BY PID CONTROLLERS

BY

ZHANG ZHIPING (B.ENG.)

DEPARTMENT OF ELECTRICAL AND
COMPUTER ENGINEERING

A THESIS SUBMITTED
FOR THE MASTER OF ENGINEERING

NATIONAL UNIVERSITY OF SINGAPORE
2007

Acknowledgments

I would like to express my sincere appreciation to my advisor, Professor Wang Qing-Guo, for his excellent guidance and gracious encouragement through my study. His uncompromising research attitude and stimulating advice helped me in overcoming obstacles in my research. His wealth of knowledge and accurate foresight benefited me in finding the new ideas. Without him, I would not be able to finish the work here.

I also want to thank Prof. Ge Shuzhi Sam, Prof. Chen Ben Mei, Prof. Sun Ji-tao, Dr. He Yong, and Dr. Lin Chong for their comments, advice, and inspiration. My special gratitude goes to my colleagues and friends. I would like to extend my thanks to Dr. Lu Xiang, Mr. Liu Min, Mr. Ye Zhen, Miss Gao Hanqiao and many others working in the Advanced Control Technology Lab. I enjoyed very much the time spent with them. I appreciate the National University of Singapore for the research facilities and scholarship.

I am very much indebted to my parents and sister for their love and support. It is impossible to thank them adequately. Instead I devote this thesis to them and hope they will find joy in my humble achievement.

Contents

List of Figures

List of Tables

Summary

The Proportional-plus-Integral-plus-Derivative (PID) controllers have found wide acceptance and applications in the industry for the past few decades(Wang *et al.*, 1999). Over 90% of controllers used in process control are of PID type (Ho and Edgar, 2004). It is known that many of the control loops are not well tuned and yield poor performance. An abundant amount of research has been conducted on tuning and applications of PID controllers. Over the years, some common beliefs, well-known formulas and tuning methods have been published. One of the common beliefs is that the integral action in PID controllers reduces the system stability. However, nobody has systematically examined its correctness. The classical PID controller tuning methods proposed by Ziegler and Nichols in 1942 (Ziegler and Nichols, 1942) include a formula $T_i = 4T_d$, which is well known in control community. Another popular and widely used PID controller tuning method is the dominant pole placement. It is to choose a pair of desired poles, which represent the requirements on the closed-loop response, and make them dominant. However, the existent design method cannot always guarantee the dominance of chosen poles and thus sometimes results in poor control performance. With these considerations in mind, this thesis is devoted to study (i) relationship on stabilizability of LTI systems by P and PI controllers; (ii) one simple PID tuning method resulting in $T_i = 4T_d$ and another method for dominant poles and phase margin; (iii) guaranteed dominant pole placement with PID controllers; (iv) internet-based control system design with PID controllers.

Firstly, the relationship on stabilizability of linear time-invariant (LTI) systems by P and PI controllers is investigated. It is found that PI is no poorer than P in terms of stabilization. PI can stabilize all the systems that P stabilizes but the converse is not true in general. The cases with the equivalence of stabilizability by P and PI are established and they are in general low-order systems with few zeros. The cases with non-equivalence are also identified.

Secondly, two simple tuning methods for PID controllers are presented. A framework for PID controller design is presented and it leads to the important popular setting, $T_i = 4T_d$ which first appeared in the Ziegler and Nichols tuning and is widely adopted today. The framework also provides some analytical PID tuning formulas with improved performance over the ZN tuning. Besides, a simple PID tuning method for dominant poles and phase margin specification is proposed. Time domain specifications such as settling time and percentage overshoot are represented by a pair of dominant poles, which are then combined with phase margin specification to achieve closed-loop stability and robustness. A graphical way is developed to determine the PID settings to meet these specifications simultaneously.

Thirdly, guaranteed dominant pole placement with PID controllers is achieved with two simple and easy methods. They are based on the Root-Locus and Nyquist plot respectively. The basic idea is that the chosen pair of poles give rise to two real equations which are solved for I and D terms via the proportional gain and the locations of all other closed-loop poles can then be studied with respect to this single variable gain. In the Root-Locus method the roots of the closed-loop characteristic equation for all the positive values of K_P are plotted and the range of K_P such that the roots other than the chosen dominant pair are all in the desired region is then determined. In the Nyquist plot method the same idea is used but the Nyquist contour is modified. If a solution exists, the parametrization of all the solutions is explicitly given. The extension of theses two methods to MIMO systems is also discussed in the decoupling framework. Together with the model reduction techniques, the multivariable PID controller is developed. Satisfactory performances are obtained in the examples.

Fourthly, a new design method for internet-based control systems in a dual-rate configuration is proposed. The design achieves load minimization and dynamic performance specifications. It avoids the complexity of large scale system design by focusing on individual control systems. In the dual-rate configuration, the plant under control is first stabilized by a local controller with a high sampling rate. The remote PID controller, which regulates the output according to the desirable reference, adopts a low sampling rate to reduce load on the network. The upper bound of the remote PID controller's sampling time which meets the requirement on control performance is derived and a simple tuning method for the remote PID controller is presented.

The results presented in the thesis have very practical value as well as sound theoretical contributions. The findings in the thesis can be applied to industrial control systems, as shown from several real-time implementation tests.

Chapter 1

Introduction

1.1 Motivation

Automatic control has played a vital role in the advance of engineering and science. It is extremely important in space-vehicle systems, missile-guidance systems, robotic systems, and so on. In addition, automatic control has become an important and integral part of modern manufacturing and industrial processes (Ogata, 2002). The key component in an automatic control system–the controller receives information from input devices and generates commands for corrective action to maintain system performance. The controller could be either a piece of hardware or software code in a computer. Over the years, development of analysis and design of controllers has been a constant goal for control engineers and great achievement has been made. Various types of controllers and advanced control schemes have been proposed and used in practice, which has improved system performance and productivity.

The Proportional-Integral-Derivative (PID) controllers have been most commonly used in automatic control systems for decades. The controller structure is simple and well understood by process engineers. It provides feedback, can eliminate steady state offsets through integral action and anticipate the future through derivative action (Astrom and Hagglund, 1995). They are fairly robust and versatile over a wide range of processes. In fact, over 90% of industrial controllers are of the PID type. Today PID control is still an active research area in control community due to its importance and the possibility for improvement. Almost all control journals including IEEE TAC and Automatica continue to publish papers on PID controllers. For example, Issue 1 in Volume 26 of IEEE Control Systems Magazine, 2006, is a special issue on PID.

As mentioned above, the PID controller can eliminate steady-state offset for step inputs through integral action. However, the integral action is widely believed to have contributed negatively to stability of the closed-loop systems due to the addition of one open-loop pole at the origin. And it is a long-standing, wide-spread, and common belief or perception that the integral control deteriorates closed-loop stability. Control engineers and researchers often think that integral action is useless for stabilization and PI control cannot do better stabilization than P control. Besides, most people in the control community think that a system which cannot be stabilized by the P controller is not stabilizable by the PI controller. However, none of these similar beliefs are fully tested or theoretically proved. In fact, a systematic answer to this stabilizability problem is lacking.

Stability is an important and fundamental requirement on system design but it is not yet sufficient for PID control applications. System performance should be always addressed. To ensure certain performance, many PID tuning methods have been proposed over the years. The classical methods of tuning PID controllers were developed by Ziegler and Nichols (1942). These methods are still widely used and often form the basis for tuning procedures used by controller manufacturers and process industry (Astrom and Hagglund, 1995). The first design method proposed by Ziegler and Nichols is based on the open-loop step response of the system. The PID parameters are directly given as functions of two parameters characterizing the open-loop step response. The second design method is also called the Ziegler-Nichols frequency response method. The design is based on knowledge of the point on the Nyquist curve of the process transfer function where the Nyquist curve intersects the negative real axis. This point is characterized by the ultimate gain and ultimate period. Ziegler and Nichols have given simple formulas for the

PID parameters in terms of the ultimate gain and ultimate period. Both of the ZN tuning methods include a formula, $T_i = 4T_d$, which is well known in control community. Many other tuning methods either use this formula or slightly modify it to $T_i = \delta T_d$(δ is a tuning parameter) (Astrom and Hagglund, 1995; Cohen and Coon, 1953; Tang *et al.*, 2002; Ogata, 2002; Astrom and Hagglund, 1984; Ang *et al.*, 2005). The formula was not explained in their original paper. To our best knowledge, nobody has given an analytical explanation for it.

System Performance is measured in either frequency domain or time domain. Phase margin and gain margin are widely used as important measures when working in the frequency domain. Phase margin is calculated as the difference between -180^o and the actual phase angle of the open-loop transfer function measured at the frequency where the magnitude of the open-loop transfer function is equal to one. Gain margin, on the other hand, is calculated as the ratio of 1 to the magnitude of the open-loop transfer function at the frequency where the phase angle of the open-loop transfer function is -180^o. Many PID tuning methods based on phase margin and gain margin were presented in the literature (Ho *et al.*, 1996; K. *et al.*, 1997; Tang *et al.*, 2002; Fung *et al.*, 1998; Lee, 2005). In Fung *et al.* (1998), a graphical method was proposed to obtain exact gain and phase margins for PI controller design. In Wang *et al.* (1999), a similar method for the PID controller was presented.

In time domain, the settling time and overshoot of the output step response are the important specifications widely used. These specifications may be transformed into a damping ratio and an undamped natural frequency, and then represented by a pair of poles. Pole placement in the state space and polynomial settings is very popular. It first chooses a pair of dominant poles and places the closed-loop poles in the desired locations in hope that all other poles are far to the left of the assigned poles. If so achieved, the closed-loop system may have good chance to meet the specifications represented by the assigned poles. To achieve arbitrary pole placement for SISO systems, the equivalent output feedback control should be at least of the plant order minus one. One difficulty with this method is that complex models lead to complex controllers. Arbitrary pole placement is otherwise difficult to achieve if one has to use a low-order output feedback controller for a high-order plant. For time-delay plants it is impossible to be done. One typical example is that in process control, PID controller is used to regulate a plant with delay.

To overcome this difficulty, one wishes to achieve dominant pole placement with PID controllers. Different from the arbitrary pole placemnt, it only positions a pair of conjugate poles which represent the requirements on the closed-loop response and tries to make all other poles have negligible effects on the control performance. One design for dominant pole placement was first introduced by P. Persson (Persson and Astrom, 1993) and further explained in Astrom and Hagglund (1995). Their method is often quite effective and well known in PID controller design (Astrom and Hagglund, 1995; Ogata, 2002). However, it works well only for plants of first or second order with small time delay. In the case of higher-order plants, their design uses the plants' simplified models, which are usually of second order plus time delay. As a result, the chosen poles might not be dominant in reality and the control performance would be unsatisfactory. In some cases, if not well handled, it could even result in sluggish response or even instability of the closed-loop.

Adding another robustness specification, like phase margin, to the above pole placement method and working directly on the actual model of the plant can probably solve this problem. With the requirement on phase margin fulfilled, it is possible to yield good control performances even if the chosen poles are not dominant. Phase margin also ensures robust stability and accommodates uncertainty in the process model used for control design. A graphical way can be developed to obtain exact solutions without introducing any other tuning parameters or approximation. Therefore, such a tuning method based on pole placement and phase margin is developed.

Another better way of solving this problem is to find some methods guaranteeing that the chosen poles are dominant. Different from the arbitrary pole placement, the method does not place other poles at specific locations but only ensures they are in some locations far to the left of the dominant poles. To the best of the authors' knowledge, no method is available in the literature to achieve that. Our idea, although it looks rather straightforward, is that the chosen pair of poles give rise to two real equations which are solved for I and D terms via the proportional gain and the locations of all other closed-loop poles can then be studied with respect to this single variable gain by means of Root-locus or Nyquist techniques. Two methods for guaranteed dominant pole placement, one based on Root-locus and the other based on Nyquist techniques, are developed.

Besides the analysis and tuning methods of PID controllers, researchers are also interested in the applications of PID controllers in new areas. Over the past two decades, major advancements in the area of communication and computer networks have taken place. This gave rise to a new paradigm in control systems analysis and design, namely Networked Control System. Many systems fall under such classification and several examples of NCSs can be found in various areas such as: automotive industry, teleautonomy, teleoperation of robots, and automated manufacturing systems (Yang, 2006; Hokayem and Abdallah, 2004; Tipsuwan and Chow, 2003). Networks enable remote data transfers and data exchanges among users, reduce the complexity in wiring connections and the costs of medias, and provide ease in maintenance. Several network protocols, such as Controller Area Network (CAN) and Profitbus for industrial control have been released. Meanwhile, extensive research has also been done on general computer networks especially the Internet. With the decreasing price, increasing speed and widespread usages, the internet-based control systems are attractive for use in control applications. Internet-based control systems have found their applications in many areas, such as telerobots, manufacturing industry, and virtual laboratories (Yang, 2006; Srivastava and Kim, 2003).

Internet-based control is a very challenging and promising research field. There are several problems to be tackled. The change of communication architecture from point-to-point to the internet introduces time-delay uncertainty between sensors, actuators and controllers. These time delays come from the time-sharing of the internet as well as the computation time required for physical signal coding and communication processing. The characteristics of time delays are usually random. Intensive research was done on stability analysis and methods to tackle instability and uncertainty. Many control methodologies were proposed in the literature (Tipsuwan and Chow, 2003; Guan and Yang, 2006). However, due to the difficult nature of this stability problem, few encouraging and simple result has found so far. Research has also been done on how the sampling time selection affects the control performance (Yu *et al.*, 2004; Lian *et al.*, 2002), but nobody has worked out how the control performance is affected by the sampling time. Furthermore, most of the design methods proposed so far are unable to meet certain requirements on control performance, such as overshoot and settling time of step response.

The stability issue is first encountered when using PID controllers in the internet-based control system design. PID controllers are usually for benign and stable processes while the internet-based control systems could easily become unstable because of the random time delay. One simple solution to this problem is to adopt a dual-rate configuration as presented in Yang and Yang (2007). Together with some simplifications, it becomes possible to use some well-established methods for PID control and propose a load minimization design method for the internet-based control systems with dynamic performance specifications.

The work in the thesis is motivated towards the development of new understanding, tuning methods and applications for PID controllers to obtain the goal of high control performance.

1.2 Contributions

In this thesis, new study on PID controllers has been carried out and their application in new areas has been implemented. In particular, this thesis investigates the following cases:

A. Relationship on stabilizability of LTI systems by P and PI Controllers

The relationship on stabilizability of linear time-invariant (LTI) systems by

P and PI controllers is investigated. It is found that PI is no poorer than P in stabilization. PI can stabilize all the systems that P stabilizes but the converse is not true in general. The cases with the equivalence of stabilizability by P and PI are established and they are in general low-order systems with few zeros. The cases with non-equivalence are also identified and presented.

B. Simple Tuning Methods for PID Controllers

Two simple tuning methods for PID controllers are presented. Firstly, a framework for PID controller design is presented which leads to the important popular and widely adopted setting, $T_i = 4T_d$ which first appeared in the Ziegler and Nichols tuning. The framework provides analytical PID tuning formulas with improved performance over the ZN tuning. Secondly, a simple PID tuning method for dominant poles and phase margin specification is proposed. Time domain specifications as settling time and overshoot of step response are represented by a pair of dominant poles, which is combined with phase margin specification to achieve closed-loop stability and robustness. A graphical way is used to determine the PID settings to meet these specifications simultaneously.

C. Guaranteed Dominant Pole Placement with PID Controllers

Guaranteed dominant pole placement with PID controllers is achieved with two simple and easy methods. They are based on Root-Locus and Nyquist plot respectively. In the Root-Locus method the roots of the closed-loop characteristic equation for all the positive values of K_P are plotted and the range of K_P such that the roots other than the chosen dominant pair are all in the desired region is then determined. In the Nyquist plot method the same idea is used but the Nyquist contour is modified. If a solution exists, the parametrization of all the solutions is explicitly given. The extension of theses two methods to MIMO systems is also discussed in the decoupling framework. Together with the model reduction techniques, the multivariable PID controller is developed. Satisfactory performances are obtained in the examples.

D. Internet-based Control Systems Design with PID Controllers

A new design method for internet-based control systems in a dual-rate configuration to achieve load minimization and dynamic performance specifications is proposed. It avoids the complexity of large scale system design by focusing on individual control systems. In the dual-rate configuration, the plant under control is first stabilized by a local controller with a high sampling rate. The remote PID controller, which regulates the output according to the desirable reference, adopts a low sampling rate to reduce load on the network. The upper bound of the remote PID controller's sampling time which meets the requirement on control performance is derived and a simple tuning method for the remote PID controller is presented.

1.3 Organization of the Thesis

This thesis is organized as follows. Chapter 1 is the introduction, followed by Chapter 2 on relationship on stabilizability of LTI systems by P and PI controllers. Chapter 3 presents two simple tuning methods for PID controllers and Chapter 4 proposes the guaranteed dominant pole placement with PID controllers. Chapter 5 is on the internet-based control systems design with PID controllers. Chapter 6 concludes this thesis.

Chapter 2

Relationship of Stabilizability by P and PI Controllers

2.1 Introduction

P and PI controllers are simple effective controllers and widely used in real life. In process control, most loops are actually PI control (Astrom and Hagglund, 1995). The integral action in PI controllers can eliminate steady-state offset, but it is believed to have contributed negatively to the stability of the closed-loop systems due to the addition of one open-loop pole at the origin. Thus, control engineers seem to think that integral action is useless for stabilization and PI control cannot do better stabilization than P control. Most people believe that a system which cannot be stabilized by the P controller is not stabilizable by the PI controller. However, this belief is not fully tested or theoretically proved. In fact, a systematic answer to this stabilizability problem is lacking. Let us address it more rigorously, the question to ask is whether there is the equivalence between stabilizability by P and PI in general. In other words, can P stabilize all the systems which PI stabilizes, and conversely, can PI stabilize all the systems that P stabilizes? This chapter aims to answer these questions and correct the common perception that the PI controller is poorer than the P controller in stabilization of the system. It is found that PI is no poorer than P in stabilization. PI can stabilize all the systems that

Table 2.1. Stabilizability Equivalence by P and PI Controllers

$G(s) = \frac{b_m s^m + b_{m-1} s^{m-1} + ... + b_1 s + b_0}{s^n + a_{n-1} s^{n-1} + ... + a_1 s + a_0}$, $b_0 \neq 0$	Equivalence
stable	$n < \infty$
unstable with no zero: $b_m = b_{m-1} = ... = b_1 = 0$	$n \leq 4$
unstable with one zero: $b_m = b_{m-1} = ... = b_2 = 0,\ b_1 \neq 0$	$n \leq 3$
unstable with two zeros: $b_2 \neq 0$	no

P stabilizes but the converse is not true in general. The stabilizability equivalence holds for all stable systems and for several types of low-order unstable systems. Non-equivalence examples are presented for complementary cases to equivalence ones. The proof for the high-order equivalent cases and search for non-equivalent examples are the most challenging and difficult part of our research. The whole picture of our research results can be seen in Table 2.1.

Please note that uncertainties of a system model in general do not affect the validity of the results in Table 2.1. The robustness or stability margin may be briefly discussed in two ways. Let us consider gain margin first. The change of gain causes no change to our results. It is readily seen by having $kG(s)$ (k is a positive real number) in Table 2.1 instead of $G(s)$, and then all the conditions hold for any k. Another simple way to consider stability robustness is to keep some common distance d of all poles from the stability boundary, the imaginary axis. Let $s = s' - d$. And we require the poles at s-plane to have their real parts less than $-d < 0$. This is equivalent to make the poles at s'-plane have their real parts less than 0. When $s = s' - d$ is substituted to $G(s)$ to transform s-plane to s'-plane, the derivations and the results of this paper are still applicable, since the numbers of zeros and poles do not change.

This chapter is organized as follows. Section 2.2 gives the problem formation and preliminaries. Sections 2.3 and 2.4 discuss the non-zero and one-zero plants respectively. Section 2.5 discusses the plants with two or more zeros and Section 2.6 is the conclusion.

2.2 Problem Formulation and Preliminaries

Consider a LTI system described by the transfer function,

$$G(s) = \frac{N(s)}{D(s)}, \tag{2.1}$$

where $N(s)$ and $D(s)$ are co-prime polynomials given by

$$N(s) = b_m s^m + b_{m-1} s^{m-1} + ... + b_1 s + b_0,$$
$$D(s) = s^n + a_{n-1} s^{n-1} + ... + a_1 s + a_0,$$

with $n \geq m$. In this chapter, we assume that $G(s)$ has no zero at $s = 0$ to avoid any unstable zero-pole cancellation with a PI controller:

$$N(0) \neq 0. \tag{2.2}$$

This assumption is necessary to address a meaningful stabilizability comparison between P and PI control because otherwise PI control can never internally stabilize a system with a zero at the origin.

The system (2.1) is controlled in the conventional unity negative output feedback configuration, as depicted in Figure 2.1.

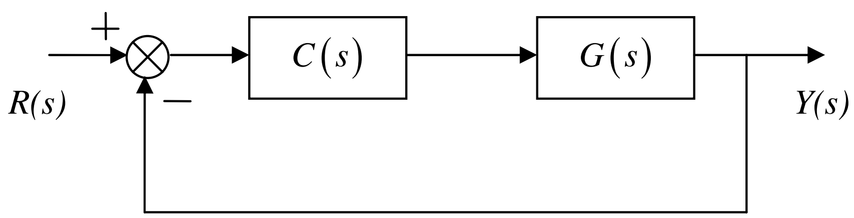

Figure 2.1. Unity output feedback control System

The controller $C(s)$ can be of P type:

$$C_P(s) = K, \tag{2.3}$$

or of PI type :

$$C_{PI}(s) = K_P + \frac{K_I}{s}, K_I \neq 0, \tag{2.4}$$

where $K_I \neq 0$ is imposed so that the latter always has non-zero integral action and P is never a special case of PI. It is to make two controllers exclusive of each other and thus stabilizability equivalence study meaningful. Please note that K, K_P and K_I could be either negative or positive. The resulting closed-loop characteristic equation is

$$D(s) + KN(s) = 0 \tag{2.5}$$

for P-control, and

$$sD(s) + (K_P s + K_I)\, N(s) = 0 \tag{2.6}$$

for PI-control.

Our problem at hand is to find the class of the system, $G(s)$, for which both equations, (2.5) and (2.6), can be made stable (having all the roots with negative real parts) by suitable choice of relevant parameters involved. If this is the case, $G(s)$ is called stabilizability-equivalent by P and PI controllers. Thus, stabilizability-equivalent cases are the systems which both P and PI can stabilize or the conditions for the stabilizability by P and PI are the same. The non-equivalent cases are the systems which P cannot stabilize but PI can, or P can stabilize but PI cannot.

For a stable system, by the Root-Locus, it is always stabilizable by P-control as long as the gain K is sufficiently small. For PI-control, let $K_P = 0$ so that it reduces to I control. A stable system with (2.2) is also stabilizable by I-control as long as $|K_I|$ is sufficiently small and $G(0)K_I > 0$. This establishes Lemma 2.1 below.

Lemma 2.1. *The class of stable systems is stabilizability-equivalent by P and PI controllers.*

Lemma 2.1 facilitates us to consider the problem for unstable systems only. For unstable systems we have established Lemma 2.2.

Lemma 2.2. *If a system given by (2.1) and (2.2) is stabilizable by a P controller, so is it by a PI controller.*

Proof. If a system given by (2.1) and (2.2) is stabilizable by a P controller, then there is some K such that the characteristic equation (2.5) is stable. The closed-loop characteristic equation with PI, (2.6), can be rewritten as

$$s\left[D(s) + KN(s)\right] + \left[\left(K_P - K\right)s + K_I\right]N(s) = 0,$$

or

$$1 + \frac{K_I}{s}\left[\frac{\left(\frac{K_P-K}{K_I}s + 1\right)N(s)}{D(s) + KN(s)}\right] = 0.$$

This can be viewed as the closed-loop characteristic equation with $\frac{K_I}{s}$ controlling the plant:

$$\frac{\left(\frac{K_P-K}{K_I}s + 1\right)N(s)}{D(s) + KN(s)},$$

which has a non-zero static gain due to (2.2) and is stable as its denominator is the same as the left side of (2.5). It follows from the Root-Locus technique that there is always a non-zero K_I such that the closed-loop is stable, that is, there also exits a PI controller stabilizing $G(s)$. This completes the proof. □

Lemma 2.2 states that stabilizability by P implies stabilizability by PI. As a result, one only needs to address the converse case: when does stabilizability by PI imply stabilizability by P. Combined with Lemma 2.1, this side of problem on stabilizability equivalence for unstable systems will be discussed in terms of the number of zeros associated with the system in the subsequent sections.

2.3 Plants with No Zero

The equivalence of stabilizability holds for a plant of up to fourth order with no zero. Because the proofs on the plants of third or lower order are relatively simple, only the proof on the fourth-order plant is presented below for the sake of demonstration. For non-equivalent cases, one example of fifth order is provided and explained.

First-order. The transfer function of the first-order system without any zero is given by

$$G(s) = \frac{b_0}{s + a_0}.$$

P control gives the closed-loop characteristic equation as

$$s + (Kb_0 + a_0) = 0, \tag{2.7}$$

which is compared with the PI case:

$$s^2 + (K_P b_0 + a_0)\, s + K_I b_0 = 0. \tag{2.8}$$

It is straightforward to see that (2.7) and (2.8) can always be made stable by P and PI controller parameters, respectively. Thus the equivalence holds.

Example 1.1. Let

$$G(s) = \frac{1}{s - 1}.$$

It can be stabilized by a P controller $C_P(s) = 2$ and also a PI controller $C_{PI}(s) = 2 + \frac{1}{s}$, respectively.

Second-order. The transfer function of the second-order system with no zero is given by

$$G(s) = \frac{b_0}{s^2 + a_1 s + a_0}.$$

The closed-loop characteristic equation with a P controller is

$$s^2 + a_1 s + (a_0 + Kb_0) = 0. \tag{2.9}$$

The stability requires

$$(i) a_1 > 0,\ (ii) a_0 + Kb_0 > 0. \tag{2.10}$$

The closed-loop characteristic equation with a PI controller is

$$s^3 + a_1 s^2 + (a_0 + K_P b_0)\, s + K_I b_0 = 0. \tag{2.11}$$

The Routh array of (2.11) is given as follows:

$$\begin{array}{lll} s^3 & 1 & a_0 + K_P b_0 \\ s^2 & a_1 & K_I b_0 \\ s^1 & a_0 + K_P b_0 - \frac{K_I b_0}{a_1} & \\ s^0 & K_I b_0 & \end{array}$$

The stability requires

$$(i) a_1 > 0,\ (ii) a_0 + K_P b_0 > 0,\ (iii) K_I b_0 > 0,\ (iv) a_0 + K_P b_0 - \frac{K_I b_0}{a_1} > 0. \quad (2.12)$$

Equation (2.12) implies (2.10) because from (2.12) we can show that (2.10) is true by letting . Therefore, PI stabilization ensures P stabilization here. The equivalence of stabilizability holds.

Example 2.2. Let

$$G(s) = \frac{1}{s^2 + s - 2}$$

It can be stabilized by a P controller $C_P(s) = 4$ and also a PI controller $C_{PI}(s) = 4 + \frac{1}{s}$, respectively.

Third-order. The transfer function of the third-order system with no zero is given by

$$G(s) = \frac{b_0}{s^3 + a_2 s^2 + a_1 s + a_0}.$$

The closed-loop characteristic equation with a P controller is

$$s^3 + a_2 s^2 + a_1 s + (a_0 + K b_0) = 0. \quad (2.13)$$

The Routh array of (2.13) is

$$\begin{array}{lll} s^3 & 1 & a_1 \\ s^2 & a_2 & a_0 + K b_0 \\ a^1 & a_1 - \frac{a_0 + K b_0}{a_2} & \\ s^0 & a_0 + K b_0 & \end{array}$$

The stability requires

$$(i) a_2 > 0,\ (ii) a_1 > 0,\ (iii) a_0 + K b_0 > 0,\ (iv) a_1 - \frac{a_0 + K b_0}{a_2} > 0. \quad (2.14)$$

The closed-loop characteristic equation with a PI controller is

$$s^4 + a_2 s^3 + a_1 s^2 + (a_0 + K_P b_0)\, s + K_I b_0 = 0. \tag{2.15}$$

The Routh array of (2.15) is given as follows:

$$\begin{array}{llll}
s^4 & 1 & a_1 & K_I b_0 \\
s^3 & a_2 & a_0 + K_P b_0 & \\
s^2 & a_1 - \frac{a_0 + K_P b_0}{a_2} & K_I b_0 & \\
s^1 & a_0 + K_P b_0 - \frac{K_I a_2 b_0}{a_1 - \frac{a_0 + K_P b_0}{a_2}} & & \\
s^0 & K_I b_0 & &
\end{array}$$

The stability requires

$$\begin{gathered}
(i) a_2 > 0,\ (ii) a_1 > 0,\ (iii) a_0 + K_P b_0 > 0,\ (iv) K_I b_0 > 0, \\
(v) a_1 - \frac{a_0 + K_P b_0}{a_2} > 0,\ (vi) a_0 + K_P b_0 - \frac{K_I a_2 b_0}{a_1 - \frac{a_0 + K_P b_0}{a_2}} > 0.
\end{gathered} \tag{2.16}$$

Suppose that (2.16) is true. Let $K = K_P$. Then,

$$\begin{gathered}
a_0 + K b_0 = a_0 + K_P b_0 > 0, \\
a_1 - \frac{a_0 + K b_0}{a_2} = a_1 - \frac{a_0 + K_P b_0}{a_2} > 0.
\end{gathered}$$

Thus, equation (2.16) implies (2.14). PI stabilization ensures P stabilization. The equivalence of stabilizability holds.

Example 2.3. Let

$$G(s) = \frac{1}{s^3 + s^2 + 5s + 6}.$$

It can be stabilized by a P controller $C_P(s) = -3$ and also a PI controller $C_{PI}(s) = -3 + \frac{1}{s}$, respectively.

Fourth-order. The transfer function of fourth-order plant with no zero is given by

$$G(s) = \frac{b_0}{s^4 + a_3 s^3 + a_2 s^2 + a_1 s + a_0},\ b_0 \neq 0.$$

The closed-loop characteristic equation with a P controller is

$$s^4 + a_3 s^3 + a_2 s^2 + a_1 s + (a_0 + K b_0) = 0. \tag{2.17}$$

The Routh array of (2.17) is given as follows:

$$\begin{array}{llll}
s^4 & 1 & a_2 & a_0+Kb_0 \\
s^3 & a_3 & a_1 & \\
s^2 & a_2-\frac{a_1}{a_3} & a_0+Kb_0 & \\
s^1 & a_1-\frac{a_3(a_0+Kb_0)}{a_2-\frac{a_1}{a_3}} & & \\
s^0 & a_0+Kb_0 & &
\end{array}$$

The stability requires

$$\begin{gathered}(i)a_3>0,(ii)a_2>0,(iii)a_1>0,(iv)a_0+Kb_0>0,\\ (v)a_2-\frac{a_1}{a_3}>0,(vi)a_1-\frac{a_3\left(a_0+Kb_0\right)}{a_2-\frac{a_1}{a_3}}>0.\end{gathered} \tag{2.18}$$

The closed-loop characteristic equation with a PI controller is

$$s^5+a_3s^4+a_2s^3+a_1s^2+\left(a_0+K_Pb_0\right)s+K_Ib_0=0. \tag{2.19}$$

The Routh array of (2.19) is

$$\begin{array}{llll}
s^5 & 1 & a_2 & a_0+K_Pb_0 \\
s^4 & a_3 & a_1 & K_Ib_0 \\
s^3 & a_3 & a_0+K_Pb_0-\frac{K_Ib_0}{a_3} & \\
s^2 & a_1-\frac{a_3\ \ a_0+K_Pb_0-\frac{K_Ib_0}{a_3}}{a_2-\frac{a_1}{a_3}} & K_Ib_0 & \\
s^1 & a_0+K_Pb_0-\frac{K_Ib_0}{a_3}-\frac{K_Ib_0\ \ a_2-\frac{a_1}{a_3}}{a_1-\frac{a_3\left(a_0+K_Pb_0-\frac{K_Ib_0}{a_3}\right)}{a_2-\frac{a_1}{a_3}}} & & \\
s^0 & K_Ib_0 & &
\end{array}$$

The stability requires

$$\begin{aligned}&(i)a_3>0,(ii)a_2>0,(iii)a_1>0,(iv)a_0+K_Pb_0>0,(v)K_Ib_0>0,(vi)a_2-\frac{a_1}{a_3}>0,\\ &(vii)a_1-\frac{a_3\left(a_0+K_Pb_0-\frac{K_Ib_0}{a_3}\right)}{a_2-\frac{a_1}{a_3}}>0,\\ &(viii)a_0+K_Pb_0-\frac{K_Ib_0}{a_3}-\frac{K_Ib_0\left(a_2-\frac{a_1}{a_3}\right)}{a_1-\frac{a_3\ \ a_0+K_Pb_0-\frac{K_Ib_0}{a_3}}{a_2-\frac{a_1}{a_3}}}>0.\end{aligned} \tag{2.20}$$

It is straightforward to see, by comparing (2.20) with (2.18), that (2.20) will imply (2.18) if one shows (iv) and (vi) of (2.18) using (2.20). Suppose that (2.20) is true. Let $K = K_P - \frac{K_I}{a_3}$. It follows from (v), (vi) and (vii) of (2.20) that

$$\frac{K_I b_0 \left(a_2 - \frac{a_1}{a_3}\right)}{a_1 - \frac{a_3 \;\; a_0 + K_P b_0 - \frac{K_I b_0}{a_3}}{a_2 - \frac{a_1}{a_3}}} > 0.$$

One then sees

$$a_0 + K b_0 = a_0 + K_P b_0 - \frac{K_I b_0}{a_3} > a_0 + K_P b_0 - \frac{K_I b_0}{a_3} - \frac{K_I b_0 \left(a_2 - \frac{a_1}{a_3}\right)}{a_1 - \frac{a_3 \;\; a_0 + K_P b_0 - \frac{K_I b_0}{a_3}}{a_2 - \frac{a_1}{a_3}}} > 0,$$

where the last equality is due to (viii) of (2.20). Besides, from (vii) of (2.20), one has

$$a_1 - \frac{a_3 \left(a_0 + K b_0\right)}{a_2 - \frac{a_1}{a_3}} = a_1 - \frac{a_3 \left(a_0 + K_P b_0 - \frac{K_I b_0}{a_3}\right)}{a_2 - \frac{a_1}{a_3}} > 0$$

Therefore, (2.18) is true as well. PI stabilization guarantees P stabilization here. The equivalence of stabilizability holds.

Example 2.4. Let

$$G(s) = \frac{1}{s^4 + s^3 + 3s^2 + s + 3}.$$

It can be stabilized by a P controller $C_P(s) = -2$ and also a PI controller $C_{PI} = -2 + \frac{0.1}{s}$, respectively.

Fifth-order. It is found that the equivalence of stabilizability by P and PI does not hold when the plant is of fifth order with no zero. This is due to the increased elements of the Routh array of the closed-loop characteristic equation. With P, one coefficient in the first column of the Routh array contains the square of K. It is thus possible that this coefficient is always non-positive for some specific plants if other coefficients in the first column are kept positive. But with PI, this coefficient could be positive due to the presence of another variable, K_I. One example, which cannot be stabilized by any P controller but can be stabilized by PI, is provided here.

Example 2.5. Let

$$G(s) = \frac{1}{s^5 + 2s^4 + 2s^3 + 3s^2 + s + 0.5}.$$

With a P controller, the closed-loop characteristic equation is

$$s^5 + 2s^4 + 2s^3 + 3s^2 + s + (0.5 + K) = 0.$$

Its Routh array is

$$\begin{array}{llll} s^5 & 1 & 2 & 1 \\ s^4 & 2 & 3 & 0.5+K \\ s^3 & 0.5 & 0.75-0.5K & \\ s^2 & 2K & 0.5+K & \\ s^1 & -\frac{(K-0.5)^2}{2K} & & \\ s^0 & 0.5+K & & \end{array}$$

Since no K exists such that $2K$ and $-\frac{(K-0.5)^2}{2K}$ are positive simultaneously, P controller cannot stabilize this system. This can be verified by the root loci of positive and negative gain, as shown in Figure 2.2. For any single value of K, no matter whether it is positive or negative, there is at least one root not in the left-half plane.

However, a PI controller

$$C_{PI}(s) = 0.5 + \frac{0.1}{s}$$

is found to be able to stabilize this system. The closed-loop characteristic equation is $s^6 + 2s^5 + 2s^4 + 3s^3 + s^2 + s + 0.1 = 0$. The poles are located at $s = -0.0478 \pm 1.0145j$, $s = -0.0229 \pm 0.7153j$, $s = -1.7505$ and $s = -0.1081$, which are all stable.

Remark 2.1. Equivalence does not hold in general. But there could be equivalent examples such as $G(s) = \frac{1}{s^5+4s^4+10s^3+10s^2+5s-1}$, which can be stabilized by a P controller $C_P(s) = 2$ and $C_{PI} = 2 + \frac{0.1}{s}$.

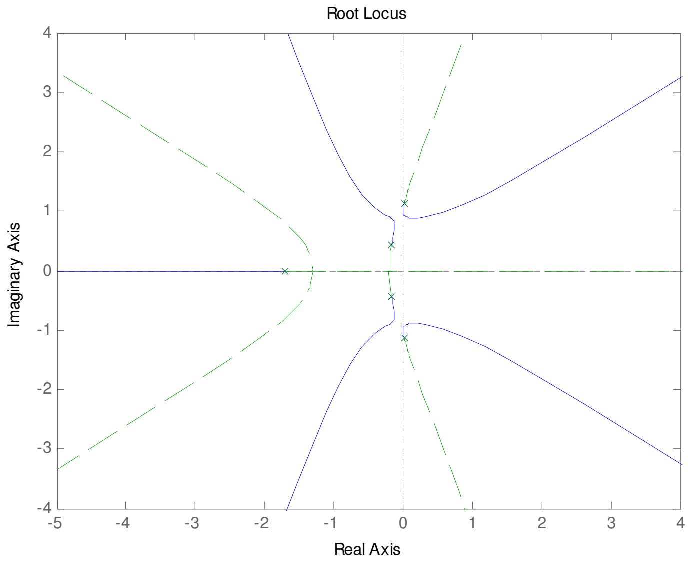

Figure 2.2. Root-Locus of $G(s)$ in Example 2.5 for positive (in solid blue lines) and negative (in dashed green lines) K

Higher-order. Consider Example 5 with the same controller but the plant being cascaded with $\frac{1}{(\alpha s+1)^m}$, where α is a small positive number and m is a positive integer. The Nyquest curve of such a new open-loop for either P or PI case can be made as close as possible to the counterpart of the original loop and thus causes no change of encirclements with respect to the critical point. The equivalence of stabilizability by P and PI fails in such cases, too.

Example 2.6. Let

$$G(s) = \frac{1}{s^5 + 2s^4 + 2s^3 + 3s^2 + s + 0.5}\left(\frac{1}{0.0001s+1}\right)^4.$$

Like $G(s)$ in Example 2.5, $G(s)$ here has two unstable poles at $s = 0.0195 \pm 1.1388j$. This plant cannot be stabilized by P controller, which can be verified by the root loci of positive and negative gain, as shown in Figure 2.3 and 2.4. Figure 2.4 is the zoom-in version focusing on the roots very near the y-axis. For any single value of K, no matter whether it is positive or negative, there is at least one root not in the left-half plane.

Nevertheless, the same PI controller in Example 2.5,

$$C_{PI}(s) = 0.5 + \frac{0.1}{s}$$

can stabilize this plant. The closed-loop poles are located at $s = -10001.0626 \pm 1.0628j$, $s = -9998.9374 \pm 1.0624j$, $s = -1.7505$, $s = -0.0228 \pm 0.7152j$ and $s = -0.1081$ which are all stable.

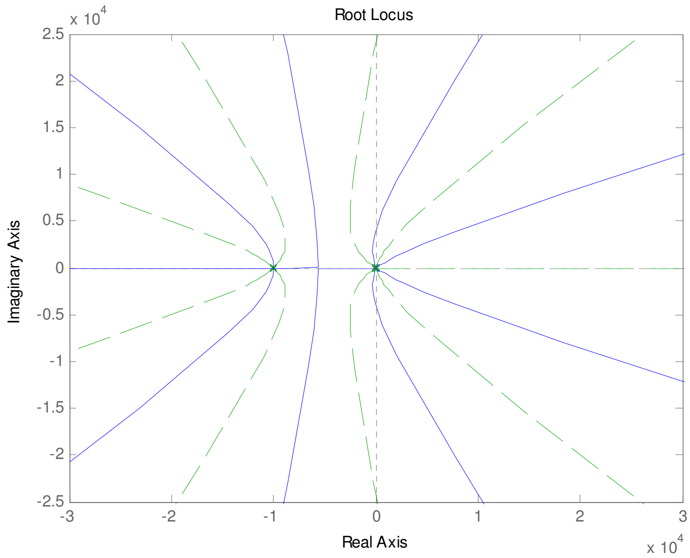

Figure 2.3. Root-Locus of $G(s)$ in Example 2.6 for positive (in solid blue lines) and negative (in dashed green lines) K

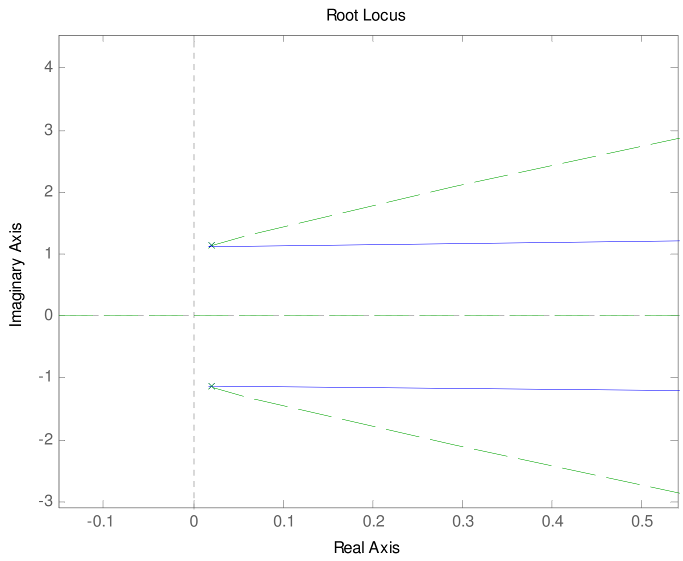

Figure 2.4. Zoomed-in Root-Locus of $G(s)$ in Example 2.6 for positive (in solid blue lines) and negative (in dashed green lines) K

Time-delay cases. For the sake of completeness, let us address the problem for time-delay plants (Gu *et al.*, 2003). In Lu (2006), five types of unstable time-delay plants of up to second order with no zero are studied and the stabilizability results are displayed in Table 2.2. All the first-order unstable plants are studied there and all the cases of up to second-order except the plants with two unstable poles, which neither P nor PI can stabilize, are also considered. From their results and our Lemma 2.2 before, one therefore concludes that the equivalence of stabilizability by P and PI holds for time-delay plants of first order and second order with no zero.

Table 2.2. Summary of some stabilizability results for time-delay plants

Plant Model	P	PI
$\frac{1}{s}e^{-Ls}$	$\forall L > 0$	$\forall L > 0$
$\frac{1}{s(s+1)}e^{-Ls}$	$\forall L > 0$	$\forall L > 0$
$\frac{1}{s-1}e^{-Ls}$	$L < 1$	$L < 1$
$\frac{1}{s(s-1)}e^{-Ls}$	none	none
$\frac{1}{(s-1)(Ts+1)}e^{-Ls}$	$L < 1 - T$	$L < 1 - T$

2.4 Plants with One Zero

In this section, the equivalence of stabilizability holds for a plant of up to third order with one zero. Two examples of higher orders are provided for non-equivalent cases.

First-order. The transfer function of the first-order system with one zero is given by

$$G(s) = \frac{b_1 s + b_0}{s + a_0}.$$

With a P controller, the closed-loop characteristic equation is

$$(1 + Kb_1)\left(s + \frac{Kb_0 + a_0}{1 + Kb_1}\right) = 0.$$

It can also be written as

$$(1 + Kb_1)\left(s + a_0 + \frac{b_0 - b_1 a_0}{\frac{1}{K} + b_1}\right) = 0.$$

There always exists a $K \neq 0$ such that the term $a_0 + \frac{b_0 - b_1 a_0}{\frac{1}{K} + b_1}$ is positive. Therefore, P controller can stabilize this kind of systems. Thus, the equivalence of stabillizability holds.

Example 2.7. Let

$$G(s) = \frac{s+1}{s-2}.$$

It can be stabilized by a P controller $C_P(s) = 5$ and also a PI controller $C_{PI}(s) = 5 + \frac{1}{s}$, respectively.

Second-order. The transfer function of the second-order delay-free unstable systems with one zero is written as

$$G(s) = \frac{b_1 s + b_0}{s^2 + a_1 s + a_0}$$

where $b_1 \neq 0$. The closed-loop characteristic equation with a P controller is

$$s^2 + (a_1 + Kb_1)\, s + (a_0 + Kb_0) = 0. \tag{2.21}$$

The stability of (2.21) requires

$$(i) a_1 + Kb_1 > 0, \;\; (ii) a_0 + Kb_0 > 0. \tag{2.22}$$

The closed-loop characteristic equation with a PI controller is

$$s^3 + (a_1 + K_P b_1)\, s^2 + (a_0 + K_I b_1 + K_P b_0)\, s + K_I b_0 = 0. \tag{2.23}$$

The Routh array of (2.23) is

$$\begin{array}{lll} s^3 & 1 & a_0 + K_I b_1 + K_P b_0 \\ s^2 & a_1 + K_P b_1 & K_I b_0 \\ s^1 & a_0 + K_I b_1 + K_P b_0 - \frac{K_I b_0}{a_1 + K_P b_1} & \\ s^0 & K_I b_0 & \end{array}$$

The stability requires

$$\begin{gathered} (i) a_1 + K_P b_1 > 0, \;\; (ii) a_0 + K_I b_1 + K_P b_0 > 0, \\ (iii) a_0 + K_I b_1 + K_P b_0 - \frac{K_I b_0}{a_1 + K_P b_1} > 0, \;\; (iv) K_I b_0 > 0. \end{gathered} \tag{2.24}$$

Suppose that (2.24) is true. Let $K = K_P + \frac{b_1}{b_0} K_I$. Then,

$$\begin{aligned} a_1 + Kb_1 &= a_1 + \left(K_P + K_I \frac{b_1}{b_0}\right) b_1 = a_1 + K_P b_1 + \left(\frac{b_1}{b_0}\right)^2 K_I b_0 > a_1 + K_P b_1 > 0, \\ a_0 + Kb_0 &= a_0 + K_P b_0 + K_I b_1 > 0. \end{aligned}$$

Therefore, PI stabilization guarantees P stabilization here. The equivalence holds.

Example 2.8. Let

$$G(s) = \frac{s+1}{s^2 + s - 2}.$$

It can be stabilized by a P controller $C_P(s) = 3$ and also a PI controller $C_{PI} = 3+\frac{1}{s}$.

Third-order. The transfer function of third-order plant with one zero is given by

$$G(s) = \frac{b_1 s + b_0}{s^3 + a_2 s^2 + a_1 s + a_0},\ b_1 \neq 0.$$

The closed-loop characteristic equation with a P controller is

$$s^3 + a_2 s^2 + (a_1 + Kb_1) + (a_0 + Kb_0) = 0. \tag{2.25}$$

The Routh array of (2.25) is

$$\begin{array}{lll} s^3 & 1 & a_1 + Kb_1 \\ s^2 & a_2 & a_0 + Kb_0 \\ s^1 & a_1 + Kb_1 - \frac{a_0+Kb_0}{a_2} & \\ s^0 & a_0 + Kb_0 & \end{array}$$

The stability requires

$$(i)a_2 > 0,\ (ii)a_1 + Kb_1 > 0,\ (iii)a_0 + Kb_0 > 0,\ (iv)a_1 + Kb_1 - \frac{a_0 + Kb_0}{a_2} > 0. \tag{2.26}$$

The closed-loop characteristic equation with a PI controller is

$$s^4 + a_2 s^3 + (a_1 + K_P b_1)\, s^2 + (a_0 + K_P b_0 + K_I b_1)\, s + K_I b_0 = 0. \tag{2.27}$$

The Routh array of (2.27) is

$$\begin{array}{llll} s^4 & 1 & a_1 + K_P b_1 & K_I b_0 \\ s^3 & a_2 & a_0 + K_P b_0 + K_I b_1 & \\ s^2 & a_1 + K_P b_1 - \frac{a_0+K_P b_0+K_I b_1}{a_2} & & \\ s^1 & a_0 + K_P b_0 + K_I b_1 - \frac{K_I a_2 b_0}{a_1 + K_P b_1 - \frac{a_0+K_P b_0+K_I b_1}{a_2}} & & \\ s^0 & K_I b_0 & & \end{array}$$

The stability requires

$$\begin{aligned} &(i)a_2 > 0,\ (ii)a_1 + K_P b_1 > 0,\ (iii)a_0 + K_P b_0 + K_I b_1 > 0, \\ &(iv)K_I b_0 > 0,\ (v)a_1 + K_P b_1 - \frac{a_0 + K_P b_0 + K_I b_1}{a_2} > 0, \\ &(vi)a_0 + K_P b_0 + K_I b_1 - \frac{K_I a_2 b_0}{a_1 + K_P b_1 - \frac{a_0+K_P b_0+K_I b_1}{a_2}} > 0. \end{aligned} \tag{2.28}$$

Suppose that (2.28) is true. Let $K = \frac{K_P b_0 + K_I b_1}{b_0}$. Then,

$$\begin{aligned}
a_1 + K b_1 &= a_1 + K_P b_1 + K_I b_0 \left(\frac{b_1}{b_0}\right)^2 > a_1 + K_P b_1 > 0, \\
a_0 + K b_0 &= a_0 + K_P b_0 + K_I b_1 > 0, \\
a_1 + K b_1 - \frac{a_0 + K b_0}{a_2} &= a_1 + K_P b_1 - \frac{a_0 + K_P b_0 + K_I b_1}{a_2} + K_I b_0 \left(\frac{b_1}{b_0}\right)^2 \\
&> a_1 + K_P b_1 - \frac{a_0 + K_P b_0 + K_I b_1}{a_2} > 0.
\end{aligned}$$

Therefore, PI stabilizabtion also ensures P stabilization here. The equivalence holds here.

Example 2.9. Let

$$G(s) = \frac{s-1}{s^3 + s^2 + 5s + 6}.$$

It can be stabilized by a P controller $C_P(s) = -4$ and also a PI controller $C_{PI}(s) = -4 - \frac{1}{s}$.

Fourth-order. The equivalence of stabilizability by P and PI does not hold when the system is of fourth order. Similar to the case of the fifth-order with no zero, with P or PI, one coefficient in the first column of the Routh array contains the square of K or K_P. For certain plants, it is possible that if other coefficients in the first column are positive this coefficient is always non-positive with P but could be positive with PI due to the presence of another variable, K_I. Example 10 is provided here for demonstration.

Example 2.10. Let

$$G_{10}(s) = \frac{s-1}{s^4 + s^3 + 3s^2 + s + 3}.$$

With a P controller, the closed-loop characteristic equation is

$$s^4 + s^3 + 3s^2 + (K+1)\,s + (3-K) = 0.$$

Its Routh array is

$$\begin{array}{llll}
s^4 & 1 & 3 & 3-K \\
s^3 & 1 & K+1 & \\
s^2 & 2-K & 3-K & \\
s^1 & \frac{(K-1)^2}{K-2} & & \\
s^0 & 3-K & &
\end{array}$$

Since no K exists such that $2 - K$ and $\frac{(K-1)^2}{K-2}$ are positive simultaneously, P controller cannot stabilize the system. It can be further verified by the root loci of both positive and negative, as shown in Figure 2.5. For any single value of K, no matter whether it is positive or negative, there is at least one root not in the left-half plane.

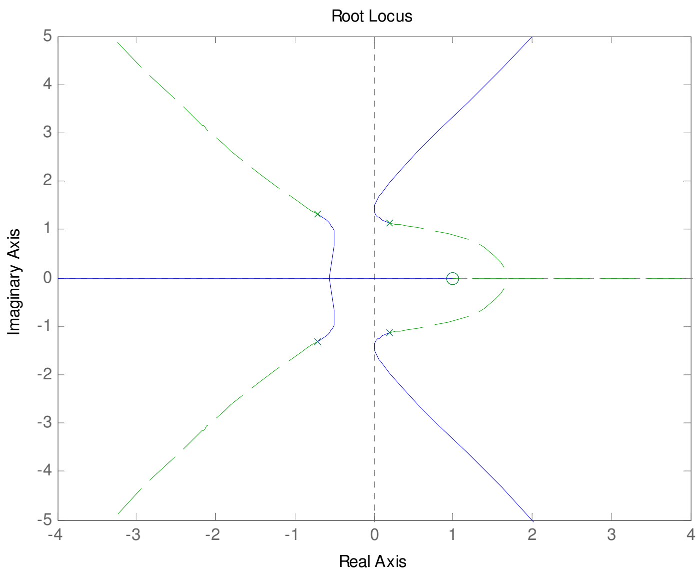

Figure 2.5. Root-Locus of $G(s)$ in Example 2.10 for positive (in solid blue lines) and negative (in dashed green lines) K

On the other hand, a simple PI controller

$$C_{PI} = 1 - \frac{0.5}{s}$$

can stabilize the system. The closed-loop characteristic equation is

$$s^5 + s^4 + 3s^3 + 2s^2 + 1.5s + 0.5 = 0.$$

The poles are, $s = -0.1267 \pm 1.4562j$, $s = -0.1561 \pm 0.7172j$ and $s = -0.4344$, which are all located in the left-half plane.

Higher-order. Consider Example 2.10 with the same controller but the plant being cascaded with $\frac{1}{(\alpha s+1)^m}$, where α is a small positive number and m is a positive integer. The Nyquest curve of such a new open-loop for either P or PI case can be made as close as possible to the counterpart of the original loop and thus causes no change of encirclements with respect to the critical point. The equivalence of P and PI stabilizability fails in such cases, too.

Example 2.11. Let

$$G(s) = \frac{s-1}{s^4+s^3+3s^2+s+3}\left(\frac{1}{0.0001s+1}\right)^4.$$

$G(s)$ has two unstable poles at $s = 0.2030 \pm 1.1449j$. This plant cannot be stabilized by P controller, which is verified by the root-loci of positive and negative gain, in Figure 2.6 and 2.7. Figure 2.7 is the zoom-in version focusing on the roots very near the y-axis. For any single value of K, no matter whether it is positive or negative, there is at least one root not in the left-half plane.

Nevertheless, the same PI controller in Example 2.10,

$$C_{PI}(s) = 1 - \frac{0.5}{s}$$

can stabilize this plant. The closed-loop poles are located at $s = -10009.9954$, $s = -10000.0075 \pm 10.0028j$, $s = -9989.9897$, $s = -0.1265 \pm 1.4561j$, $s = -0.1562 \pm 0.7170j$ and $s = -0.4346$, which are all stable.

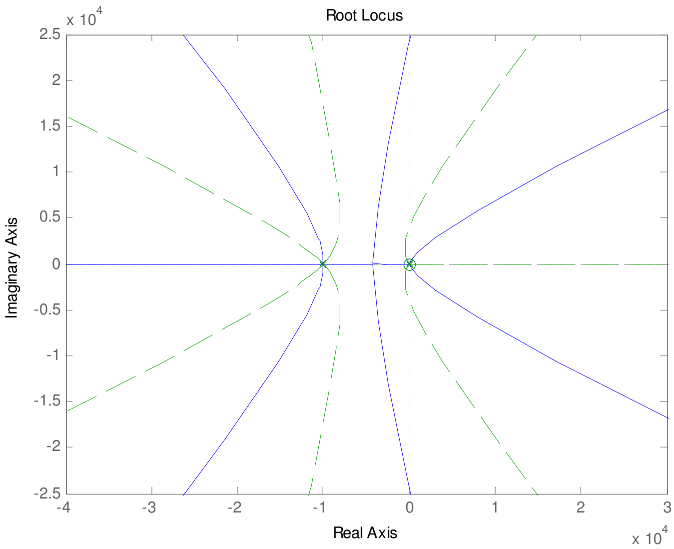

Figure 2.6. Root-Locus of $G(s)$ in Example 2.11 for positive (in solid blue lines) and negative (in dashed green lines) K

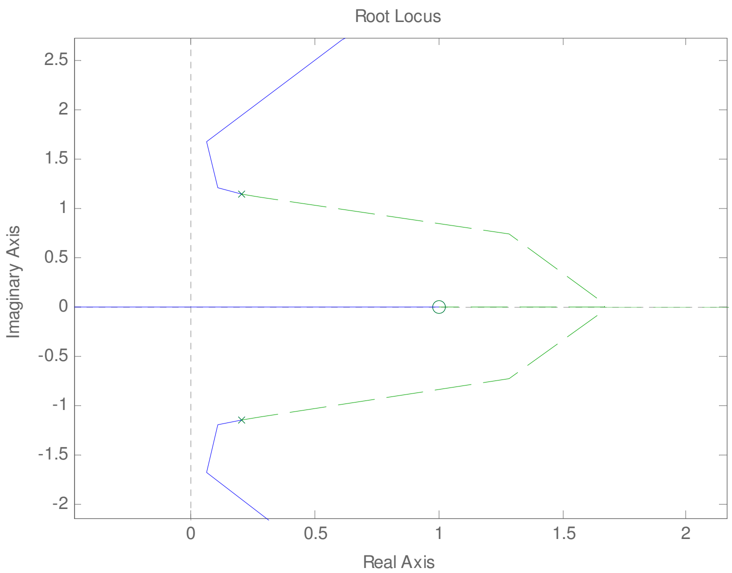

Figure 2.7. Zoomed-in Root-Locus of $G(s)$ in Example 2.11 for positive (in solid blue lines) and negative (in dashed green lines) K

2.5 Plants with Two or More Zeros

It is found that the equivalence of stabilizability by P and PI does not hold in general for a plant with two or more zeros. A different approach has been taken to search for the non-equivalent example. Based on the Routh's Stability Criterion, all the parameters in the closed-loop characteristic equation should be positive in order to have stability of the closed-loop system. When the term of s does not exist in both the denominator and nominator of the open-loop system transfer function, there would be no way for P to stabilize the system but it is possible for PI to stabilize, since PI has an s term but P does not. We have found two examples of non-equivalent cases for demonstration, one at second-order and the other at third order.

Example 2.12. Let

$$G(s) = \frac{s^2+1}{s^2+2}.$$

With a P controller, the closed-loop characteristic equation is

$$(K+1)\,s^2 + (2K+1) = 0. \tag{2.29}$$

Equation (2.29) lacks the term of s, so it always have roots located in the right-half plane or at the imaginary-axis regardless of what K is chosen. P controller cannot stabilize the system. It can be further verified by the root loci of both positive and negative gains, as shown in Figure 2.8. For any single value of K, no matter whether it is positive or negative, there is at least one root not in the left-half plane.

However, a PI controller, such as,

$$C_{PI}(s) = 1 + \frac{1}{s}$$

can stabilize the system. Its closed-loop characteristic equation is

$$2s^3 + s^2 + 3s + 1 = 0. \tag{2.30}$$

The roots of (2.30) are $s = -0.0772 \pm 1.2003j$ and $s = -0.3456$, all located in the left-half plane.

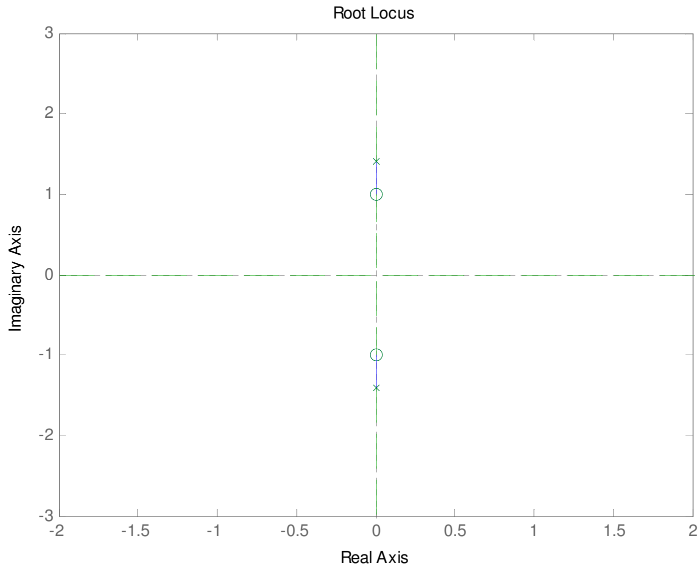

Figure 2.8. Root-Locus of $G(s)$ in Example 2.12 for positive (in solid blue lines) and negative (in dashed green lines) K

Example 2.13. Let

$$G(s) = \frac{s^2 + 0.1}{s^3 - 0.3s^2 - 0.016}.$$

With a P controller, the closed-loop characteristic equation is

$$s^3 + (K_P - 0.3)\, s^2 + (0.1K_P - 0.016) = 0. \tag{2.31}$$

Similarly, Equation (2.31) lacks the term of s, thus P controller cannot stabilize the system. It can be further verified by the root loci of both positive and negative gains. We find that a PI controller,

$$C_{PI}(s) = 0.5 + \frac{0.5}{s}$$

can stabilize the system. The closed-loop characteristic equation is

$$s^4 + 0.2s^3 + 0.5s^2 + 0.034s + 0.05 = 0.$$

The poles are $s = -0.0865 \pm 0.5888j$ and $s = -0.0135 \pm 0.3755j$, all located in the left-half plane.

Plants of higher order and with more zeros. Consider Example 3 again with the plant being cascaded with $\frac{(\beta s+1)^l}{(\alpha s+1)^m}$, where α and β are some small positive numbers, l and m are positive integers. The Nyquest curve of such a new open-loop for either P or PI case can be made as close as possible to the counterpart of the original loop and thus causes no change of encirclements with the critical point. Therefore, the conclusion drawn in Example 3 holds for the plant of higher order or with more zeros, that is, PI may stabilize but P cannot. The equivalence of stabilizability by P and PI fails in such cases as well.

Example 2.14. Let

$$G(s) = \frac{s^2+1}{s^2+2}\left(\frac{0.001s+1}{0.002s+1}\right).$$

With a P controller, the closed-loop characteristic equation is

$$(0.002+0.001K)\,s^3 + (1+K)\,s^2 + (0.004+0.001K)\,s + (2+K) = 0. \quad (2.32)$$

According to the Root-Loci of positive and negative gains, in Figure 2.9 and 2.10, Equation (2.32) always has some of its roots located in the right-half plane or at the imaginary-axis for any value of K.

However, a PI controller, such as,

$$C_{PI}(s) = 1 + \frac{1}{s}$$

can stabilize the system, since its closed-loop characteristic equation,

$$0.003s^4 + 2.001s^3 + 1.005s^2 + 3.001s + 1 = 0,$$

has the roots at $s = -666.4996$, $s = -0.0773 \pm 1.2003j$ and $s = -0.3457$, all in the left-half plane.

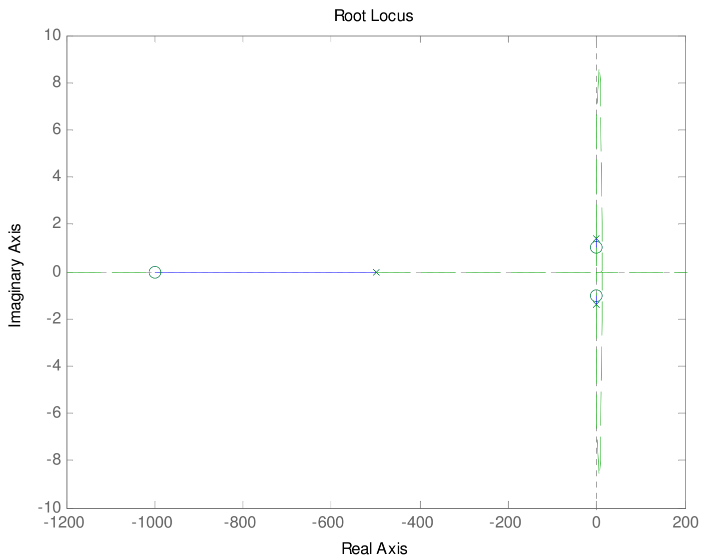

Figure 2.9. Root-Locus of $G(s)$ in Example 2.14 for positive (in solid blue lines) and negative (in dashed green lines) K

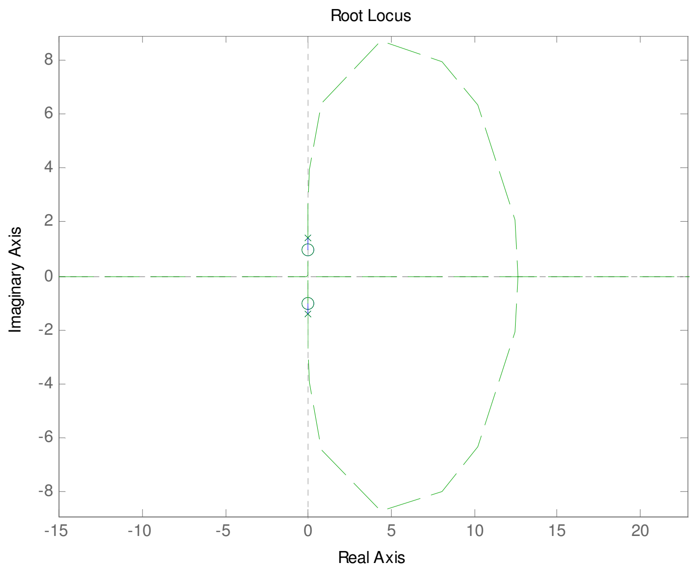

Figure 2.10. Zoomed-in Root-Locus of $G(s)$ in Example 2.14 for positive (in solid blue lines) and negative (in dashed green lines) K

2.6 Conclusion

In this chapter, the relationship on stabilizability of LTI systems by P and PI controllers is studied. It is shown that the equivalence of stabilizability by P and PI holds for the classes of (i)stable plants, (ii)plants of up to fourth order with no zero, (iii)plants of up to third order with one zero. The equivalence fails for other classes of plants in general and non-equivalent examples are provided.

Chapter 3

Simple Tuning Methods for PID Controllers

3.1 Preview

After discussing the relationship of stabilizability by P and PI controllers in Chapter 2, Chapter 3 is focused on tuning of PID controllers. The fist section proposes a tuning method which leads to the famous formula $T_i = 4T_d$. In the second section another tuning method for dominant poles and phase margin is proposed.

3.2 Why $T_i = 4T_d$ for PID Controller Tuning?

3.2.1 Introduction

Among hundreds of PID tuning rules reported in the literature, one presented by Ziegler and Nichols in 1942 (Ziegler and Nichols, 1942) is still among the most famous and applicable ones. The ZN tuning includes a formula, $T_i = 4T_d$, which is well known in control community. Many other tuning methods either use this formula or slightly modify it to $T_i = \delta T_d$(δ is a tuning parameter) (Astrom and Hagglund, 1995; Cohen and Coon, 1953; Tang *et al.*, 2002; Ogata, 2002; Astrom and Hagglund, 1984; Ang *et al.*, 2005). The formula was not explained in their original paper and looks a bit mysterious. To our best knowledge, nobody has given an analytical explanation for it. It was an incidence that when we designed a framework for PID design which results in $T_i = 4T_d$. Our objective in this section is to present this framework and the corresponding tuning formula with improved performance.

3.2.2 Why $T_i = 4T_d$

Consider a process with its transfer function, $G(s)$. Suppose that $G(s)$ is non-integral and $G(0)$ is finite and positive. The process is controlled in the conventional unity feedback configuration by a PID controller of interacting form,

$$C(s) = K'\left(1 + \frac{1}{sT_i'}\right)(1 + sT_d'). \tag{3.1}$$

This form is most common in commercial PID controllers (Astrom and Hagglund, 1995). It is re-written in the standard version,

$$C(s) = K_P\left(1 + \frac{1}{T_i s} + T_d s\right), \; K_P > 0, \; T_i > 0, \; T_d > 0, \tag{3.2}$$

which has to satisfy

$$T_i - 4T_d \geq 0 \tag{3.3}$$

in order to fit into the format of (3.1). Typically, control system design specifications include the percentage overshoot and settling time/rising time in time domain, which may be represented by a pair of dominant poles (Ogata, 2002): $p_{1,2} = -\alpha \pm j\beta, \; \alpha > 0, \; \beta > 0$. Besides, one may also wish to minimize regulation error. Let us take the integral error (Astrom and Hagglund, 1995): $IE = \int_0^\infty e(t)dt$, where $e(t)$ is the error between the step set-point and the resultant output response. In order to make IE meaningful, the dominant poles, i.e. $p_{1,2} = -\alpha \pm j\beta$, chosen should be lightly-damped or close to the critically-damped case. Our PID controller design objective is to find the PID settings such that the IE is minimized subject to $p_{1,2} = -\alpha \pm j\beta$ being the poles of the resultant closed-loop system.

Since $p_1 = -\alpha + j\beta$ should be a pole of the closed-loop, it satisfies the following characteristic equation: $1 + C(p_1)G(p_1) = 0$, which, after taking real and imaginary parts, $Re[\ ]$ and $Im[\ ]$, become $K_P\left[\frac{1}{T_i}-\alpha\left(\alpha^2-\beta^2\right)T_d\right]$ and $K_P\left(\beta-2\alpha\beta T_d\right)=Im\left[-\frac{P_1}{G(p_1)}\right]$. They are solved to get

$$T_d=\frac{1}{2\alpha}-\frac{Im\left[-\frac{p_1}{G(p_1)}\right]}{2\alpha\beta K_P}, \tag{3.4}$$

$$T_i=\frac{K_P}{Re\left[\frac{-p_1}{G(p_1)}\right]+\frac{\alpha^2-\beta^2}{2\alpha\beta}Im\left[-\frac{p_1}{G(p_1)}\right]+\frac{\alpha^2+\beta^2}{2\alpha}K_P}. \tag{3.5}$$

It follows from the final-value theorem that

$$\begin{aligned} IE &= \lim_{t\to\infty}\int_0^t e(t)dt=\lim_{t\to\infty}E(s)=\lim_{t\to\infty}\frac{1}{sG(s)C(s)}=\frac{1}{G(0)\frac{K_P}{T_i}} \\ &= \frac{1}{G(0)\left\{Re\left[\frac{-p_1}{G(p_1)}\right]+\frac{\alpha^2-\beta^2}{2\alpha\beta}Im\left[-\frac{p_1}{G(p_1)}\right]+\frac{\alpha^2+\beta^2}{2\alpha}K_P\right\}}. \end{aligned} \tag{3.6}$$

The greater K_P is, the smaller the IE is. But allowable K_P is limited by (3.3).

Substituting (3.4) and (3.5) into (3.3) and solving the resulting inequality with respect to K_P gives

$$\begin{aligned} &\frac{1}{\beta}Im\left[-\frac{p_1}{G(p_1)}\right]-\frac{\alpha}{\beta^2}Re\left[-\frac{p_1}{G(p_1)}\right]-\frac{\alpha}{\beta^2}\sqrt{Re^2\left[-\frac{p_1}{G(p_1)}\right]+Im^2\left[-\frac{p_1}{G(p_1)}\right]}\le K_P \\ &\le\frac{1}{\beta}Im\left[-\frac{p_1}{G(p_1)}\right]-\frac{\alpha}{\beta^2}Re\left[-\frac{p_1}{G(p_1)}\right]+\frac{\alpha}{\beta^2}\sqrt{Re^2\left[-\frac{p_1}{G(p_1)}\right]+Im^2\left[-\frac{p_1}{G(p_1)}\right]}. \end{aligned}$$

The IE specification is minimized when K_P takes its maximum value in the above range:

$$K_P=\frac{1}{\beta}Im\left[-\frac{p_1}{G(p_1)}\right]-\frac{\alpha}{\beta^2}Re\left[-\frac{p_1}{G(p_1)}\right]+\frac{\alpha}{\beta^2}\sqrt{Re^2\left[-\frac{p_1}{G(p_1)}\right]+Im^2\left[-\frac{p_1}{G(p_1)}\right]}. \tag{3.7}$$

Substituting (3.7) into (3.4) and (3.5) gives

$$T_i=\frac{2\left\{\sqrt{Re^2\left[-\frac{p_1}{G(p_1)}\right]+Im^2\left[-\frac{p_1}{G(p_1)}\right]}-Re\left[-\frac{p_1}{G(p_1)}\right]\right\}}{\beta Im\left[-\frac{p_1}{G(p_1)}\right]-\alpha Re\left[-\frac{p_1}{G(p_1)}\right]+\alpha\sqrt{Re^2\left[-\frac{p_1}{G(p_1)}\right]+Im^2\left[-\frac{p_1}{G(p_1)}\right]}}, \tag{3.8}$$

$$T_d=\frac{\sqrt{Re^2\left[-\frac{p_1}{G(p_1)}\right]+Im^2\left[-\frac{p_1}{G(p_1)}\right]}-Re\left[-\frac{p_1}{G(p_1)}\right]}{2\left\{\beta Im\left[-\frac{p_1}{G(p_1)}\right]-\alpha Re\left[-\frac{p_1}{G(p_1)}\right]+\alpha\sqrt{Re^2\left[-\frac{p_1}{G(p_1)}\right]+Im^2\left[-\frac{p_1}{G(p_1)}\right]}\right\}}, \tag{3.9}$$

which obviously gives $T_i = 4T_d$.

Now consider positiveness of three PID parameters. From (3.7), $K_P > 0$ is equivalent to

$$\frac{Im\left[-\frac{p_1}{G(p_1)}\right]}{\sqrt{Re^2\left[-\frac{p_1}{G(p_1)}\right] + Im^2\left[-\frac{p_1}{G(p_1)}\right]} - Re\left[-\frac{p_1}{G(p_1)}\right]} > -\frac{\alpha}{\beta}. \tag{3.10}$$

One can verify from (3.4) and (3.5) that $K_P > 0$ implies $T_i > 0$ as well as $T_d > 0$. The condition (3.10) is used to check if the chosen specifications/closed-loop poles are achievable with PID control.

3.2.3 PID Tuning

It is straightforward to obtain from the preceding section the following PID tuning procedure:

1) Specify a pair of desired dominant poles of a closed loop system, $p_{1,2}$, according to the given specifications;

2) Check if (3.10) is true;

3) Calculate K_P and T_d by (3.7) and (3.9), respectively, and let $T_i = 4T_d$ if yes; otherwise, go to Step 1 to relax the specifications.

Example 3.1 is provided below to illustrate the design procedure in detail.

Example 3.1. Consider a high-order process,

$$G_1(s) = \frac{1}{(s+1)^8}.$$

Suppose that the specifications are the overshot of 15% and the settling time of 20s. The corresponding poles are obtained via some approximation formulae (Ogata, 2002) as $p_{1,2} = -0.2028 \pm j0.3331$. In this case, (3.10) is true and the resulting PID controller is $C(s) = 0.6468\left(1 + \frac{1}{5.2002s} + 1.3001s\right)$. Comparison is made with the ZN tuning which yields $C(s) = 1.1304\left(1 + \frac{1}{7.576s} + 1.894s\right)$ and modified ZN tuning of Astrom and Hagglund method (Astrom and Hagglund, 1984) with phase margin of $\phi_m = \frac{\pi}{4}$ which gives $C(s) = 1.3246\left(1 + \frac{1}{11.6438s} + 2.911s\right)$. Step set-point and disturbance responses are shown in Figure 3.1. The proposed method yields better performance owing to good control of closed-loop poles.

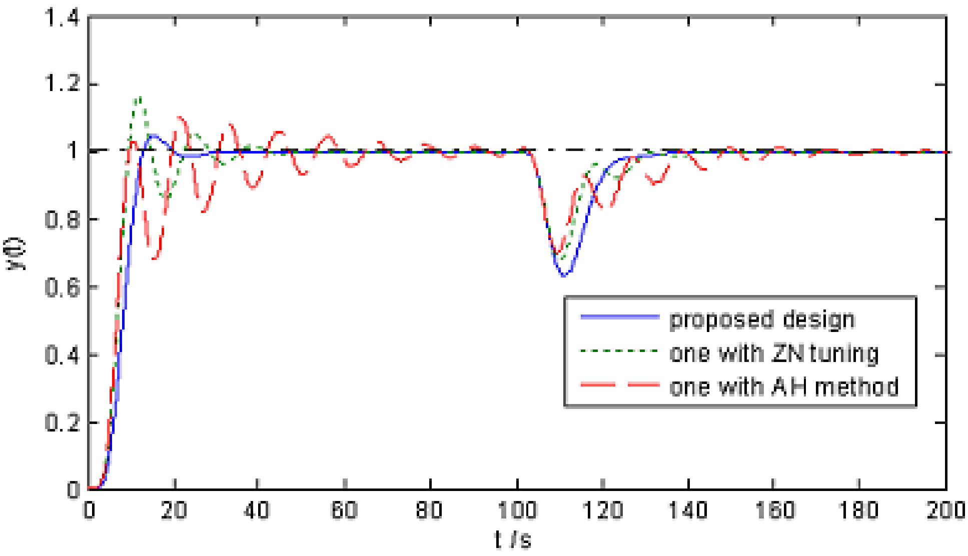

Figure 3.1. Setpoint and disturbance responses by proposed method, ZN method and AH method in Example 3.1

3.2.4 Conclusion

The popular formula, $T_i = 4T_d$, in the Z-N tuning, is obtained when the IE specification is minimized subject to some pole placement requirement. This also leads to a new analytical PID tuning with improved performance.

3.3 PID Tuning for Dominant Poles and Phase Margin

3.3.1 Introduction

In this section, a simple but effective PID tuning method for dominant poles and phase margin specifications is proposed, through employing the design idea of Lee (2005) with changes from a lead compensator to a PID controller and from the error constants to phase margin. Phase margin is included here to ensure robust stability and accommodate uncertainty in the process model used for control design. A graphical way is developed to obtain exact solutions without introducing any other tuning parameters or approximation.

The rest of this section is organized as follows. Subsection 3.3.2 presents the proposed PID design method in detail and an example is given in Subsection 3.3.3. Subsection 3.3.4 concludes the section.

3.3.2 The Proposed Method

Let a process be represented by its transfer function, $G(s)$. The process is controlled in the conventional unity feedback configuration by a PID controller,

$$C(s) = K_P + \frac{K_I}{s} + K_D s,\ K_P > 0,\ K_I > 0,\ K_D > 0. \tag{3.11}$$

Suppose that control design specifications as the settling time, rising time, peak time and/or percentage overshoot for a step input can be represented by a pair of dominant poles (Ogata, 2002):

$$p_{1,2} = -\alpha \pm j\beta,\ \alpha > 0,\ \beta > 0. \tag{3.12}$$

One should be aware that the existent dominant pole placement method cannot guarantee the assigned poles to be dominant(Astrom and Hagglund, 1995). In fact, a system with time delay has an infinite spectrum (infinite poles) and thus it is not feasible to determine dominance either analytically or numerically. However, in practice, if the poles or equivalently specifications are given reasonably, they are achievable by PID controller and the resulting performance will be close to the given specifications. That implies that the designed system behaves similarly to the one with chosen poles as dominant. In that sense, the dominant pole placement is achieved. This argument is essentially a post-check of pole dominance by examining closeness of the designed control system to the desired one.

To insure performance and robustness, we use the phase margin as another design specification. The phase margin, ϕ_m, in the standard engineering practice, is usually chosen to meet $0 < \phi_m < \frac{\pi}{2}$. Our design objective is then to determine the PID controller such that (3.12) are the poles (hopefully dominant) of the closed-loop system, and the open-loop system, $C(s)G(s)$, has the specified phase margin, ϕ_m.

One substitutes one of the two dominant poles, p_1, into the characteristic equation of the closed loop system:

$$1 + C(p_1) G(p_1) = 0,$$

which breaks into real and imaginary parts,

$$K_I - K_P\alpha + K_D\left(\alpha^2 - \beta^2\right) = Re\left[-\frac{p_1}{G(p_1)}\right], \tag{3.13}$$

$$K_P\beta - 2\alpha\beta K_D = Im\left[-\frac{p_1}{G(p_1)}\right], \tag{3.14}$$

where $Re[\,]$ and $Im[\,]$ denote the real and imaginary parts of the complex number inside the bracket. It follows from the phase margin definition that

$$G(j\omega_g) C(j\omega_g) = -e^{j\phi_m},$$

where ω_g is the gain crossover frequency of the open loop system $G(s)C(s)$. Similarly, splitting it into its real and imaginary parts yields

$$K_P = Re\left[-\frac{e^{j\phi_m}}{G(j\omega_g)}\right], \tag{3.15}$$

$$K_D\omega_g - \frac{K_I}{\omega_g} = Im\left[-\frac{e^{j\phi_m}}{G(j\omega_g)}\right]. \tag{3.16}$$

The solutions of (3.13)-(3.16) is bound to be finite as the number of unknowns, namely K_P, K_I, K_D and ω_g equals the number of equations. Unfortunately, it is difficult to find ω_g because of the nonlinearity of (3.15) and (3.16). Here a graphical method motivated by (Lee, 2005) is developed to determine ω_g as follows.

One sees from (3.14) and (3.15) that,

$$K_D = \frac{1}{2\alpha} Re\left[-\frac{e^{j\phi_m}}{G(j\omega_g)}\right] - \frac{1}{2\alpha\beta} Im\left[-\frac{p_1}{G(p_1)}\right]. \tag{3.17}$$

Substituting (3.15) and (3.17) into (3.13) gives

$$K_I = Re\left[-\frac{p_1}{G(p_1)}\right] + \frac{\alpha^2-\beta^2}{2\alpha\beta} Im\left[-\frac{p_1}{G(p_1)}\right] + \frac{\alpha^2+\beta^2}{2\alpha} Re\left[-\frac{e^{j\phi_m}}{G(j\omega_g)}\right],$$

and (3.17) and (3.16) together yield

$$K_I = \frac{{\omega_g}^2}{2\alpha} Re\left[-\frac{e^{j\phi_m}}{G(j\omega_g)}\right] - \frac{{\omega_g}^2}{2\alpha\beta} Im\left[-\frac{p_1}{G(p_1)}\right] - \omega_g Im\left[-\frac{e^{j\phi_m}}{G(j\omega_g)}\right].$$

These two expressions for K_I lead us to define

$$f_1(\omega) = Re\left[-\frac{p_1}{G(p_1)}\right] + \frac{\alpha^2-\beta^2}{2\alpha\beta} Im\left[-\frac{p_1}{G(p_1)}\right] + \frac{\alpha^2+\beta^2}{2\alpha} Re\left[-\frac{e^{j\phi_m}}{G(j\omega_g)}\right], \tag{3.18}$$

$$f_2(\omega) = \frac{{\omega_g}^2}{2\alpha} Re\left[-\frac{e^{j\phi_m}}{G(j\omega_g)}\right] - \frac{{\omega_g}^2}{2\alpha\beta} Im\left[-\frac{p_1}{G(p_1)}\right] - \omega_g Im\left[-\frac{e^{j\phi_m}}{G(j\omega_g)}\right]. \tag{3.19}$$

$f_1(\omega)$ and $f_2(\omega)$ are plotted with respect to ω in the same diagram. Their intersections make (3.13)-(3.16) hold and the value of K_I can be read directly from the intersection points if there are any. Then K_D and K_P are obtained as

$$K_D = \frac{1}{\alpha^2+\beta^2}\left\{K_I - Re\left[-\frac{p_1}{G(p_1)}\right] - \frac{\alpha}{\beta} Im\left[-\frac{p_1}{G(p_1)}\right]\right\}, \tag{3.20}$$

$$K_P = \frac{2\alpha}{\alpha^2+\beta^2}\left\{K_I - Re\left[-\frac{p_1}{G(p_1)}\right] - \frac{\alpha^2-\beta^2}{2\alpha\beta} Im\left[-\frac{p_1}{G(p_1)}\right]\right\}. \tag{3.21}$$

In control engineering practice, the same sign for K_P, K_I and K_D is required. By (3.20) and (3.21), $K_D > 0$ and $K_P > 0$ requires,

$$K_I > Re\left[-\frac{p_1}{G(p_1)}\right] + \frac{\alpha}{\beta} Im\left[-\frac{p_1}{G(p_1)}\right] = K_{i1},$$

$$K_I > Re\left[-\frac{p_1}{G(p_1)}\right] + \frac{\alpha^2-\beta^2}{2\alpha\beta} Im\left[-\frac{p_1}{G(p_1)}\right] = K_{i2},$$

so K_I must meet

$$K_I > max\{0,\ K_{i1},\ K_{i2}\}. \tag{3.22}$$

If there is no intersection of $f_1(\omega)$ and $f_2(\omega)$, it means that PID controllers cannot achieve the required specifications. In other words, the required specifications are unreasonable. One has to relax the specifications subsequently, usually by simply increasing settling time. The computation should be re-done with the relaxed specifications and the curves are to be drawn then.

When there are multiple intersection points of $f_1(\omega)$ and $f_2(\omega)$, solutions which do not meet the constraint of (3.22) are to be ignored and the one with minimum frequency should be chosen. It is because a relative lower work frequency is expected in process control practice. If there is no intersection between $f_1(\omega)$ and $f_2(\omega)$ satisfying (3.22), it means that no PID controller can meet the specifications. In this case, the desired dominant poles or phase margin specifications need to be altered to allow for the intersections satisfying the constraint of (3.22) exists.

The design procedure for PID controller is thereby summarized as:

1) Specify the phase margin and obtain a pair of desired dominant poles of a closed loop system, $p_{1,2}$, according to the prescribed time domain performance indexes such as overshoot, settling time or other specifications by some formulae from rules of thumb (Shen, 2001);

2) Plot $f_1(\omega)$ and $f_2(\omega)$ according to (3.18) and (3.19);

3) Obtain the value of K_I from the intersection points of $f_1(\omega)$ and $f_2(\omega)$ which meets (3.22), and calculate K_D and K_P by (3.20) and (3.21).

3.3.3 An example

Example 3.2. Consider a stable high order process quoted as the first example in (Fung *et al.*, 1998):

$$G(s) = \frac{1}{(s+1)^4}.$$

It is required that the overshot is not larger than 10% and the 2% settling time is less than 15s. This leads to a pair of dominant poles as $p_{1,2} = -0.2751 \pm 0.3753j$ via some approximation formulae 3.20. Take the phase margin as $\phi_m = 60^o$, as normally used in practice. We plot $f_1(\omega)$ and $f_2(\omega)$ in Figure 3.2, and a suitable intersection point, which has the lowest frequency and makes K_D as well as K_P positive, is found.

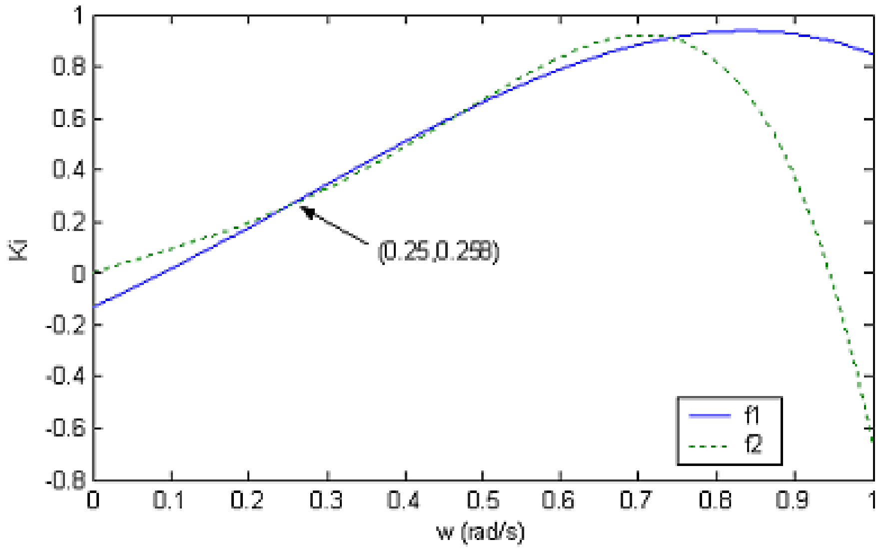

Figure 3.2. Plots of $f_1(\omega)$ and $f_2(\omega)$ in Example 3.2

The PID controller is thus obtained as

$$C(s) = 0.4969\left(1 + \frac{1}{1.926s} + 0.1534s\right).$$

Comparison is made with Fung's (Fung *et al.*, 1998) and Ziegler-Nichols method. For Fung's method, with gain and phase margins set as 3.0 and 60^o , the PI controller is obtained as $C(s) = 0.848+\frac{0.297}{s}$. For ZN method, the critical oscillation period and gain are $T_{cr} = 6.2832$ and $K_{cr} = 4$, respectively, and a PID controller is obtained as $C(s) = 2.4\left(1 + \frac{1}{3.1416s} + 0.7854s\right)$. Output time response to the unit step set-point at t=0 and step disturbance of magnitude of 0.5 at $t = 50s$ are exhibited in Figure 3.3. The proposed controller yields satisfactory performance.

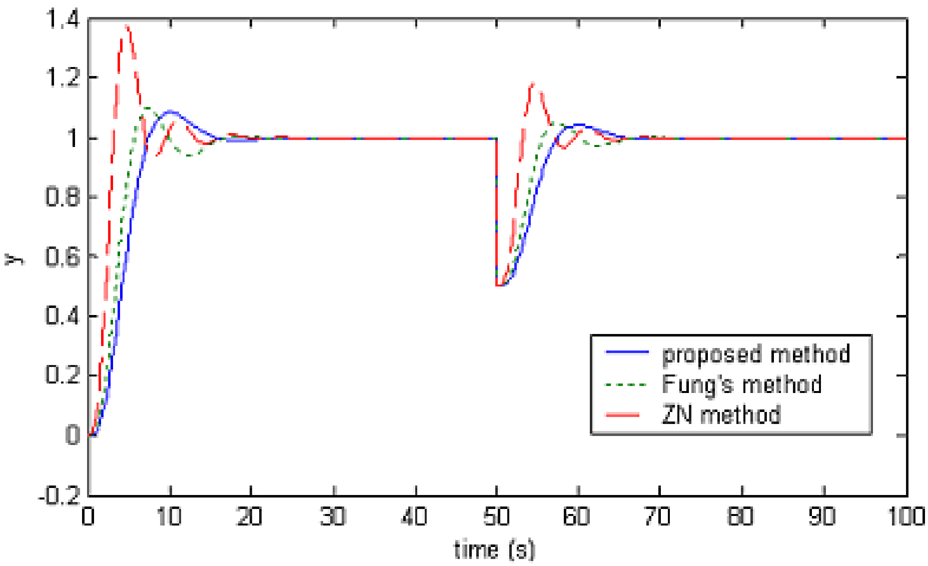

Figure 3.3. Setpoint and disturbance responses in nominal case by proposed method, Fung's method and ZN method in Example 3.2

3.3.4 Conclusion

A simple but effective PID tuning method for dominant poles and phase margin specification has been presented in this section. The method transforms the problem of solving a set of nonlinear coupled equations into finding the intersection point of two graphs plotted using the frequency response information of the process. The solvability of the problem is related to the existence and the number of the intersection points of the two graphs. However, it is noted that selection of the pair of desired dominant poles is critical as it affects solvability of the problem and deviation of actual performance from expectation

Chapter 4

Guaranteed Dominant Pole Placement with PID Controllers

4.1 Introduction

Dominant pole placement design was first introduced by P. Persson (Persson and Astrom, 1993) and further explained in Astrom and Hagglund (1995). Their methods are based on a simplified model of plants and thus cannot always guarantee the chosen poles are indeed dominant in reality. In the case of high-order plants or plants with time delay, the conventional dominant pole placement design, if not well handled, could result in sluggish response or even instability of the closed-loop. To the best of the authors' knowledge, no method is available in the literature to guarantee the dominance of the assigned poles in the above case.

The last chapter discusses a method to solve this problem by adding phase margin in the design but the performance is still not guaranteed. It is thus desirable to find out ways to ensure the dominance of chosen poles and also the closed-loop stability. This chapter aims to present some methods which provide guaranteed dominant pole placement with PID controllers. The common idea behind our methods is that the chosen pair of poles give rise to two real equations which are solved for I and D terms via the proportional gain and the locations of all other closed-loop poles can then be studied with respect to this single variable gain by means of Root-locus or Nyquist techniques. Hence, two methods for guaranteed dominant pole placement with PID controller are naturally developed.

The rest of the chapter is organized as follows. Section 4.2 states the problem and preliminary. Sections 4.3 and 4.4 each present a method along with illustrating examples. Section 4.5 is the extension to MIMO systems and Section 4.6 concludes the chapter.

4.2 Problem Statement and Preliminary

Consider a plant described by its transfer function,

$$G(s) = \frac{N(s)}{D(s)} e^{-sL}, \tag{4.1}$$

where $N(s)/D(s)$ is a proper and co-prime rational function. A PID controller in the form of

$$C(s) = K_P + \frac{K_I}{s} + K_D s$$

is used to control the plant in the conventional unity output feedback configuration.

The closed-loop characteristic equation is

$$1 + C(s)G(s) = 0. \tag{4.2}$$

The closed-loop transfer function is

$$H(s) = \frac{N(s)\left(K_D s^2 + K_P s + K_I\right)}{D(s)s + N(s)e^{-Ls}\left(K_D s^2 + K_P s + K_I\right)} e^{-Ls}. \tag{4.3}$$

Suppose that the requirements of the closed-loop control performance in frequency or time domain are converted into a pair of conjugate poles (Astrom and Hagglund, 1995):

$$\rho_{1,2} = -a \pm bj. \tag{4.4}$$

Their dominance requires that the ratio of the real part of any of other poles to $-a$ exceeds m (m is usually 3 to 5) and there are no zeros nearby. Thus, we want all other poles to be located at the left of the line of $s = -ma$, that is, the desired

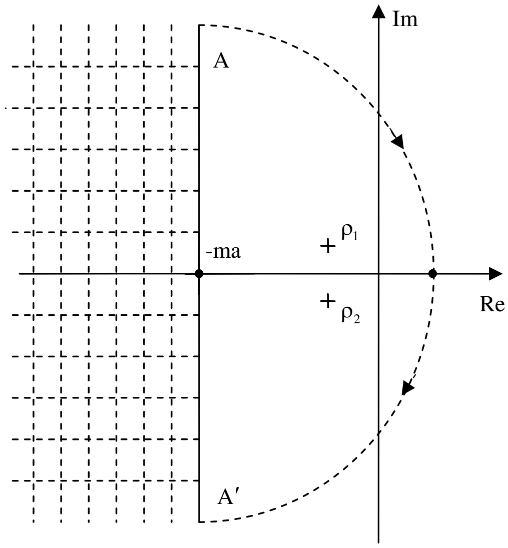

Figure 4.1. Desired region(hatched) of other poles

region as hatched in Figure 4.1. The problem of the guaranteed dominant pole placement is to find the PID parameters such that all the closed-loop poles lie in the desired region except the dominant poles, $\rho_{1,2}$.

Substitute $\rho_1 = -a + bj$ into (4.2):

$$K_P + \frac{K_I}{-a+bj} + K_D(-a+bj) = -\frac{1}{G(\rho_1)},$$

which is a complex equation. Solving the two equations given by its real and imaginary parts for K_I and K_D in terms of K_P yields

$$\begin{cases} K_I = \frac{a^2+b^2}{2a} K_p - (a^2+b^2)\, X_1, \\ K_D = \frac{1}{2a} K_p + X_2, \end{cases} \tag{4.5}$$

where

$$X_1 = \frac{1}{2b}\mathbf{Im}\left[\frac{-1}{G(\rho_1)}\right] + \frac{1}{2a}\mathbf{Re}\left[\frac{-1}{G(\rho_1)}\right], X_2 = \frac{1}{2b}\mathbf{Im}\left[\frac{-1}{G(\rho_1)}\right] - \frac{1}{2a}\mathbf{Re}\left[\frac{-1}{G(\rho_1)}\right].$$

This simplifies the original problem to a one-parameter problem for which well known methods like Root-locus and Nyquist plot are applicable now.

4.3 Root-Locus Method

The root-locus method is to show movement of the roots of the characteristic equation for all values of a system parameter. We plot the roots of the closed-loop characteristic equation for all the positive values of K_P and determine the range of K_P such that the roots other than the chosen dominant pair are all in the desired region.

Substituting (4.5) into (4.2) yields

$$1+X_2\frac{N(s)e^{-Ls}}{D(s)}s-\left(a^2+b^2\right)X_1\frac{N(s)e^{-Ls}}{D(s)s}+K_P\frac{N(s)e^{-Ls}}{D(s)}\frac{s^2+2as+(a^2+b^2)}{2as}=0. \tag{4.6}$$

Dividing both sides by the terms without K_P gives:

$$1+K_P\overline{G}(s)=0, \tag{4.7}$$

where

$$\overline{G}(s)=\frac{N(s)\left[s^2+2as+(a^2+b^2)\right]e^{-Ls}}{2aD(s)s+2aX_2N(s)s^2e^{-Ls}-2a\left(a^2+b^2\right)X_1N(s)e^{-Ls}}. \tag{4.8}$$

It can be easily verified that the manipulation does not change the roots. Two examples are provided below to prove that.

Example 4.1. Consider a fourth-order process,

$$G(s)=\frac{1}{(s+1)^2(s+5)^2}.$$

If the overshoot is to be less than 5% and the rising time less than 2.5 s, the corresponding dominant poles are $\rho_{1,2}=-0.6136\pm0.6434j$. Equation (4.5) becomes

$$\begin{cases} K_I=0.6442K_P-0.1847, \\ K_D=0.8149K_P-12.4627. \end{cases}$$

And it follows from (4.6) that

$$1+\frac{12.4627s}{(s+1)^2(s+5)^2}-\frac{0.1847}{s(s+1)^2(s+5)^2}+K_P\frac{s^2+1.227s+0.7905}{1.227s(s+1)^2(s+5)^2}=0,$$

$$\frac{s(s+1)^2(s+5)^2+12.4627s^2-0.1847}{s(s+1)^2(s+5)^2}+K_P\frac{s^2+1.227s+0.7905}{1.227s(s+1)^2(s+5)^2}=0,$$

$$\frac{1.227\left[s(s+1)^2(s+5)^2+12.4627s^2-0.1847\right]+K_P(s^2+1.227s+0.7905)}{1.227s(s+1)^2(s+5)^2}=0,$$

$$\frac{1.227s^5+14.73s^4+56.45s^3+58.33s^2+30.68s-0.2267+K_P(s^2+1.227s+0.7905)}{1.227s(s+1)^2(s+5)^2}=0.$$

While (4.7) gives

$$1+K_P\frac{s^2+1.227s+0.7905}{1.227s^5+14.73s^4+56.45s^3+58.33s^2+30.68s-0.2267}=0,$$

$$\frac{1.227s^5+14.73s^4+56.45s^3+58.33s^2+30.68s-0.2267+K_P(s^2+1.227s+0.7905)}{1.227s^5+14.73s^4+56.45s^3+58.33s^2+30.68s-0.2267}=0.$$

It is observed that (4.6) and (4.7) have the same roots or zeros but their poles are different.

Example 4.2. Consider a third-order delay process

$$G(s)=\frac{1}{(s+1)(s+10)^2}e^{-0.2s}.$$

If the overshoot is to be less than 5% and the 2%-settling time less than 7 s, the dominant poles are $\rho_{1,2}=-0.6051\pm 0.6345j$. Equation (4.5) becomes

$$\begin{cases} K_I=0.6352K_P+44.8739,\\ K_D=0.8264K_P-30.1640.\end{cases}$$

Similarly, it follows from (4.6) that

$$1-\frac{30.16s}{(s+1)(s+10)^2}e^{-0.2s}+\frac{44.87}{s(s+1)(s+10)^2}e^{-0.2s}+K_P\frac{s^2+1.2102s+0.7687}{1.2102s(s+1)(s+10)^2}e^{-0.2s}=0,$$

$$\frac{s(s+1)(s+10)^2-30.16s^2e^{-0.2s}+44.87e^{-0.2s}}{s(s+1)(s+10)^2}+K_P\frac{(s^2+1.2102s+0.7687)\,e^{-0.2s}}{1.2102s(s+1)(s+10)^2}=0,$$

$$\frac{1.2102\left[s(s+1)(s+10)^2-30.16s^2e^{-0.2s}+44.87e^{-0.2s}\right]+K_P(s^2+1.2102s+0.7687)\,e^{-0.2s}}{1.2102s(s+1)(s+10)^2}=0.$$

Equation (4.7) gives

$$1+K_P\frac{(s^2+1.2102s+0.7687)\,e^{-0.2s}}{1.2102\left[s(s+1)(s+10)^2-30.16s^2e^{-0.2s}+44.87e^{-0.2s}\right]}=0,$$

$$\frac{1.2102\left[s(s+1)(s+10)^2-30.16s^2e^{-0.2s}+44.87e^{-0.2s}\right]+K_P(s^2+1.2102s+0.7687)\,e^{-0.2s}}{1.2102\left[s(s+1)(s+10)^2-30.16s^2e^{-0.2s}+44.87e^{-0.2s}\right]}=0.$$

Please note again that only the poles have changed.

Let us continue to present our method. If $G(s)$ has no time-delay term, $\overline{G}(s)$ is a proper rational transfer function since the degrees of its nominator and denominator of $\overline{G}(s)$ equal those of the closed-loop transfer function's nominator and denominator, respectively. The root locus of (4.7) can easily be drawn with Matlab as K_P varies. The interval of K_P for guaranteed dominant pole placement can be determined from the root locus. Example 4.3 shows the design procedure in detail.

Example 4.3. Consider a fourth-order process,

$$G(s) = \frac{1}{(s+1)^2(s+5)^2}.$$

If the overshoot is to be less than 5% and the rising time less than 2.5 s, the corresponding dominant poles are $\rho_{1,2} = -0.6136 \pm 0.6434j$. Equation (4.5) becomes

$$\begin{cases} K_I = 0.6442K_P - 0.1847, \\ K_D = 0.8149K_P - 12.4627. \end{cases}$$

And it follows from (4.8) that

$$\overline{G}(s) = \frac{s^2 + 1.227s + 0.7905}{1.227s^5 + 14.73s^4 + 56.45s^3 + 58.33s^2 + 30.68s - 0.2267}.$$

The root-locus of $\overline{G}(s)$ is exhibited in Figure 4.2 with the solid lines while the edge of the desired region with $m = 3$ is indicated with dashed lines. Note that $\overline{G}(s)$ is of 5-th order and has five branches of root loci, of which two are fixed at the dominant poles while the other three move with the gain. From the root-locus, two intersection points corresponding to root locus entering into and departing from the desired region are located and give the gain range of $K_P \in (36, 51)$, which ensures all other three poles in the desired region. Besides, the positiveness of K_D and K_I requires $K_P > 15.2935$. Taking the joint solution of these two, we have $K_P \in (36, 51)$. If $K_P = 50$ is chosen, the PID controller is

$$C(s) = 50 + \frac{32.0233}{s} + 28.2832s.$$

The zeros of the closed-loop system are at $s = -0.8839 \pm 0.5934j$, which are not near the dominant poles. Figure 4.3 shows the step response of the closed-loop system.

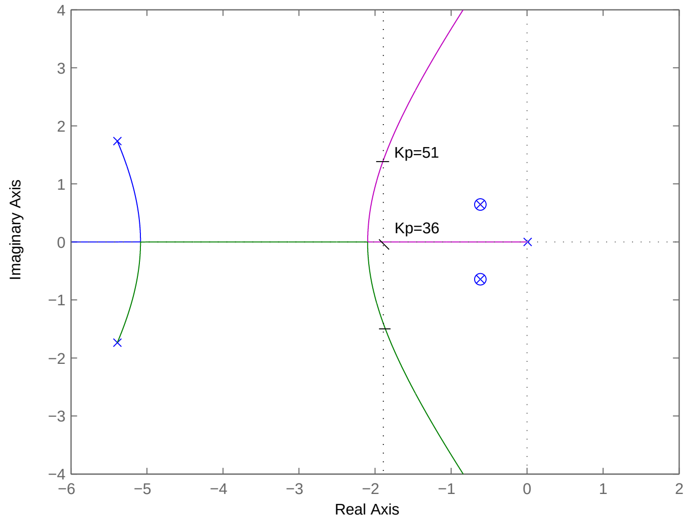

Figure 4.2. Root-Locus for Example 4.3

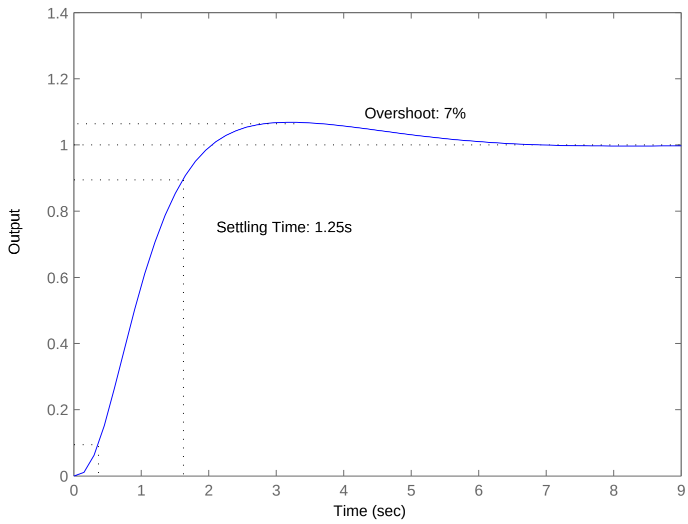

Figure 4.3. Closed-loop step response for Example 4.3

4.4 Nyquist Plot Method

If $G(s)$ has time delay, so will be $\overline{G}(s)$. Then, drawing the root locus for it could be difficult and checking locations of infinite poles is a forbidden task. Note that the Nyquist plot works well for delay systems. The Nyquist stability criterion determines the number of unstable closed-loop poles based on the Nyquist plot and the open-loop unstable poles. We use the same idea but have to modify the conventional Nyquist contour. The Modified Nyquist contour is obtained by shifting the conventional Nyquist contour to the left by ma, as Figure 4.1 shows. The image of G(s) when s traverses the modified Nyquist contour is called the modified Nyquist plot. The number of poles located outside the desired region plays the same role as that of unstable poles in the standard Nyquist criterion.

Rewrite (4.7) as

$$\tfrac{1}{K_P} + \overline{G}(s) = 0. \tag{4.9}$$

It always has $\rho_{1,2}$ as its two roots by our construction. These two lie outside the desired region. We want no more to ensure dominant pole placement. Equivalently, we want the modified Nyquist plot of $\overline{G}(s)$ to have the number of clockwise encirclements with respect to $(-\tfrac{1}{K_P}, 0)$ equal to 2 minus the number of poles of $\overline{G}(s)$ outside the desired region. This condition will determine the interval of K_P such that roots of (4.9) other than two dominant poles are in the desired region.

To find the poles of $\overline{G}(s)$ located outside the desired region, note that they are simply the roots of its denominator. Thus, we construct another characteristic equation from the denominator of $\overline{G}(s)$ in (4.8) as follows:

$$1 + \overline{G}_o(s) = 0, \tag{4.10}$$

where

$$\overline{G}_o(s) = \frac{X_2 N(s) s^2 - (a^2 + b^2)\, X_1 N(s)}{D(s) s} e^{-Ls}.$$

$\overline{G}_o(s)$ has its rational part with the degrees of its nominator and denominator being equal to those of the open-loop transfer function's nominator and denominator, respectively. The number of the roots of (4.10), that is, poles of $\overline{G}(s)$ lying outside the desired region, equals the number of clockwise encirclements of the modified Nyquist plot of $\overline{G}_o(s)$ with respect to $(-1,0)$, plus the number of poles of $\overline{G}_o(s)$ located outside the desired region. The latter is easy to find from the known denominator of $\overline{G}_o(s)$, which is, $D(s)s$.

The design procedure is summarized as follows.

Step 1. Find the poles of $\overline{G}_o(s)$ (the roots of $D(s)s$) outside the desired region and name its total number as $P^+_{\overline{G}_o}$;

Step 2. Draw the modified Nyquist plot of $\overline{G}_o(s)$, count the number of clockwise encirclements with respect to the $-1+j0$ point as $N^+_{\overline{G}_o}$, and obtain the number of poles of $\overline{G}(s)$ outside the desired region as $P^+_{\overline{G}} = N^+_{\overline{G}_o} + P^+_{\overline{G}_o}$;

Step 3. Draw the modified Nyquist plot of $\overline{G}(s)$ and find the range of K_P during which the clockwise encirclements with respect to the $(-\frac{1}{K_P}, 0)$ is 2-$P^+_{\overline{G}}$.

We now provide examples to illustrate the design procedure in detail.

Example 4.4. Consider a third-order delay process

$$G(s) = \frac{1}{(s+1)(s+10)^2}e^{-0.2s}.$$

If the overshoot is to be less than 5% and the 2%-settling time less than 7 s, the dominant poles are $\rho_{1,2} = -0.6051 \pm 0.6345j$. (4.5) becomes

$$\begin{cases} K_I = 0.6352K_P + 44.8739, \\ K_D = 0.8264K_P - 30.1640. \end{cases}$$

We have

$$\overline{G}(s) = \frac{(s^2 + 1.2102s + 0.7687)\, e^{-0.2s}}{1.2102\, [s(s+1)(s+10)^2 - 30.16s^2e^{-0.2s} + 44.87e^{-0.2s}]},$$

$$\overline{G}_o(s) = \frac{-30.16s^2 + 44.87}{s(s+1)(s+10)^2}e^{-0.2s}.$$

Take $m = 5$. We have $ma = 3.0255$ and $s = 0, -1$ as two poles of $\overline{G}_o(s)$ which are outside the desired region and $P^+_{\overline{G}_o} = 2$. Figure 4.4 is the modified Nyquist plot of $\overline{G}_o(s)$ and there is one clockwise encirclement with respect to the point $(-1,0)$, that is, $N^+_{\overline{G}_o} = 1$. Therefore, $\overline{G}(s)$ has three poles located in the desired region since $P^+_{\overline{G}} = N^+_{\overline{G}_o} + P^+_{\overline{G}_o} = 3$. It means the modified Nyquist plot of $\overline{G}(s)$ should have its clockwise encirclement with respect to the point $(-1/K_P, 0)$, equal to $2 - P^+_{\overline{G}} = -1$, that is one net anti-clockwise encirclement, for two assigned poles to dominate all others. Figure 4.5 shows the modified Nyquist plot of $\overline{G}(s)$, from which $-1/K_P \in (-0.0756, -0.0094)$ is determined to have one anti-clockwise encirclement. The positiveness of K_D and K_I requires $K_P > 36.5005$. Therefore, we have the joint solution as $K_P \in (36.5005, 106.3830)$. If $K_P = 100$ is chosen, the PID controller is

$$C(s) = 100 + \frac{108.3971}{s} + 52.4730s.$$

The zeros of the closed-loop system are at $s = -0.9529 \pm 1.0760j$, which are not near the dominant poles. Figure 4.6 shows the step response of the closed-loop system.

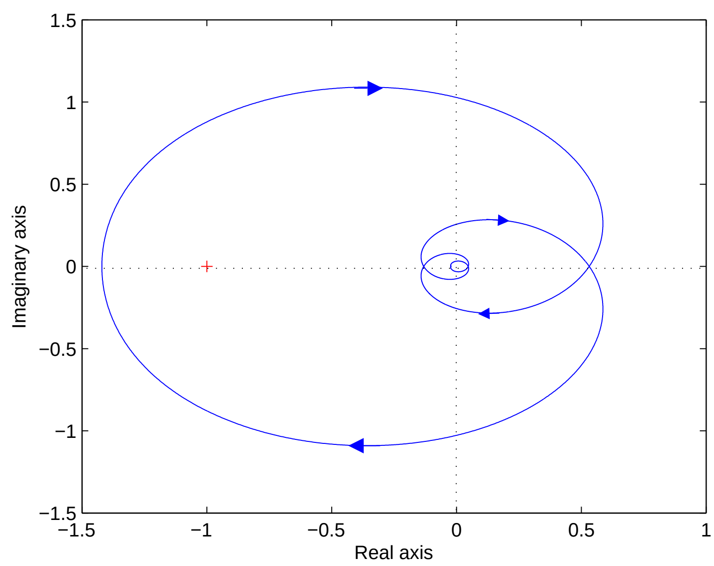

Figure 4.4. Modified nyquist plot of $\overline{G}_o$ for Example 4.4

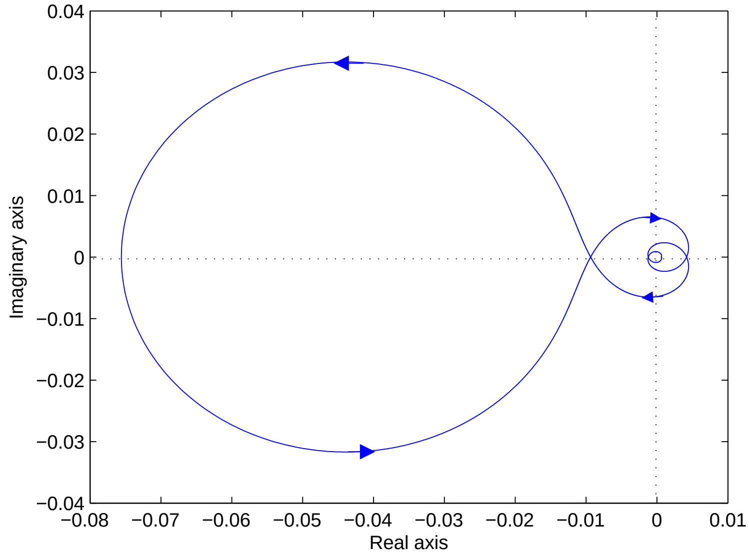

Figure 4.5. Modified nyquist plot of $\overline{G}$ for Example 4.4

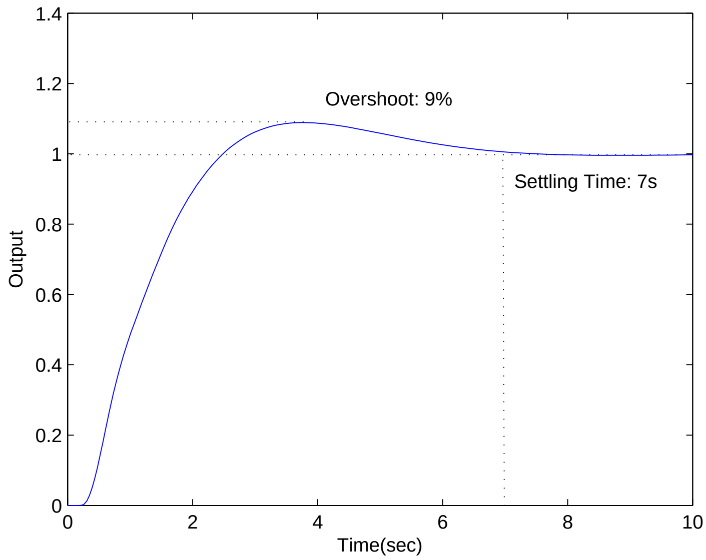

Figure 4.6. Closed-loop step response for Example 4.4

Example 4.5. Consider a highly oscillatory process

$$G(s) = \frac{1}{s^2 + s + 5} e^{-0.1s}.$$

If the overshoot is to be not larger than 10% and the 2%-settling time to be less than 15 s, the dominant poles are $\rho_{1,2} = -0.2751 \pm 0.3754j$. Equation (4.5) becomes

$$\begin{cases} K_I = 0.3937 K_P + 1.8773, \\ K_D = 1.8173 K_P + 7.7760. \end{cases}$$

We have

$$\overline{G}(s) = \frac{(s^2 + 0.5502s + 0.2166)\, e^{-0.1s}}{0.5502\, [s(s^2 + s + 5) + 7.776 s^2 e^{-0.1s} + 1.877 e^{-0.1s}]},$$

$$\overline{G}_o(s) = \frac{7.776 s^2 + 1.877}{s(s^2 + s + 5)} e^{-0.1s}.$$

Take $m = 3$. We have $ma = 0.8253$ and all three poles of $\overline{G}_o(s)$ outside the desired region and $P^+_{\overline{G}_o} = 3$. Figure 4.7 is the modified Nyquist plot of $\overline{G}_o(s)$ and there is one anti-clockwise encirclement of the point $(-1, 0)$, that is, $N^+_{\overline{G}_o} = -1$. Therefore, $\overline{G}(s)$ has two poles located in the desired region since $P^+_{\overline{G}} = N^+_{\overline{G}_o} + P^+_{\overline{G}_o} = 2$. It means the modified Nyquist plot of $\overline{G}(s)$ should have its clockwise encirclement with respect to the point $(-1/K_P, 0)$, equal to $2 - P^+_{\overline{G}} = 0$, that is zero net encirclement, for two assigned poles to dominate all others. Figure 4.8 shows the modified Nyquist plot of $\overline{G}(s)$, from which $-1/K_P \in (-\infty, -0.2851)$ is determined to have zero clockwise encirclement. A positive K_P could always make K_D and K_I positive. Therefore, we have the joint solution as $K_P \in (0, 3.5075)$. If $K_P = 1$ is chosen, the PID controller is

$$C(s) = 1 + \frac{2.2709}{s} + 9.5933s.$$

The zeros of the closed-loop system are at $s = -0.0521 \pm 0.4837j$, which are not near the dominant poles. Figure 4.9 shows the step response of the closed-loop system.

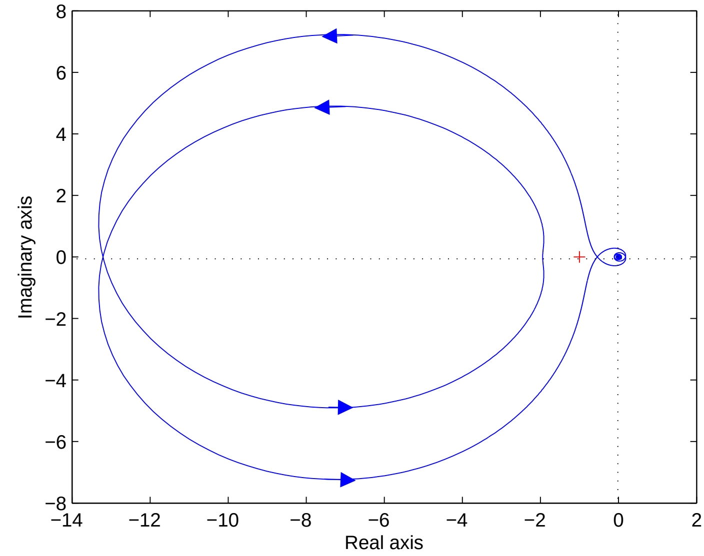

Figure 4.7. Modified nyquist plot of $\overline{G}_o$ for Example 4.5

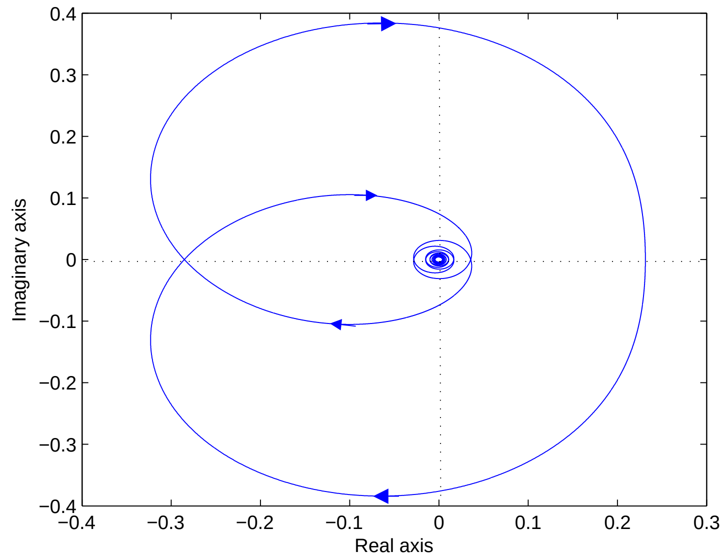

Figure 4.8. Modified nyquist plot of $\overline{G}$ for Example 4.5

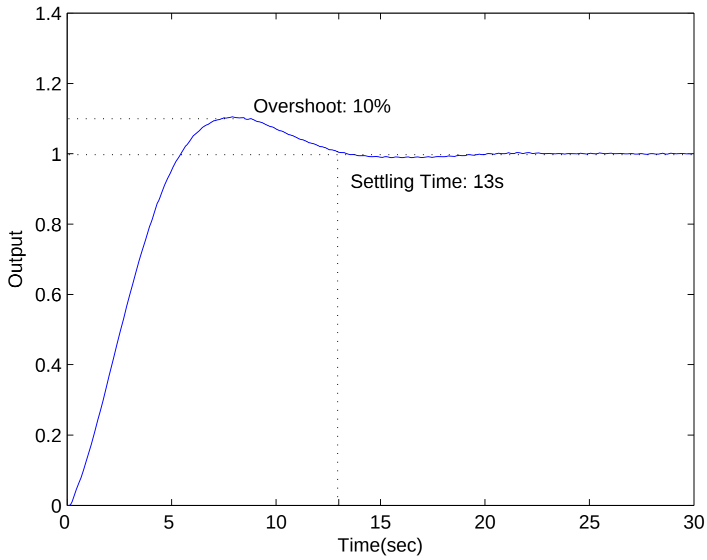

Figure 4.9. Closed-loop step response for Example 4.5

4.5 Extension to MIMO Systems

Many industrial systems are multivariable in nature. Therefore, it is of great interest and value to extend the guaranteed dominant pole placement method to the multivarible PID controller design. The multivariable systems should be decoupled first and the proposed methods can then be applied to the elements of the decoupled loop. Same as the SISO case, the Root-locus method is applied to the systems without time delay and the Nyquist plot method is applied to the time-delay systems. Because of the coupling, the multivariable controller first designed is not yet a PID controller and some model reduction techniques are used to obtain the multivariable PID controller.

Let $G(s) = [g_{ij}(s)]$ be the $m \times m$ multivarible system, $C(s) = [c_{ij}(s)]$ be the multivarible controller directly designed, the multivariable PID controller be $\hat{C}(s)$. Our goal is to get $\hat{C}(s)$ for the control system.

To overcome the effects of cross-coupled interactions, a decoupler, $D(s) = [d_{ij}(s)]$, is designed first. Using the method proposed in Wang (2003), we have

$$d_{ji}(s) = \frac{G^{ij}(s)}{G^{ii}(s)} d_{ii}(s), \tag{4.11}$$

and $Q(s) = G(s)D(s)$ becomes

$$Q(s) = diag\{q_{ii}(s)\} = diag\left\{\frac{|G(s)|}{G^{ii}(s)}d_{ii}(s)\right\},$$

where $G^{ij}(s)$ is cofactor corresponding to $g_{ij}(s)$ in $G(s)$. When elements in $Q(s)$ are complicated with time-delay or irrational, we apply the model reduction techniques based on step tests (Wang and Zhang, 2001) to obtain rational and proper estimates of $Q(s)$, which is denoted as $\hat{Q}(s)$. Thereby, the MIMO system is divided into m SISO systems, $q_{ii}(s)$ or $\hat{q}_{ii}(s)$. The methods proposed in Section 3 and 4 can be applied to design the controller for $q_{ii}(s)$ $\hat{q}_{ii}(s)$. After we have designed the PID controller,

$$k_{ii}(s) = K_{Pii} + \frac{K_{Iii}}{s} + K_{Dii}s,\ i = 1, ..., m,$$

for $q_{ii}(s)$ or $\hat{q}_{ii}(s)$, the multivariable controller $C(s)$,

$$c_{ij}(s) = d_{ij}(s)k_{jj}(s), \tag{4.12}$$

is obtained. The model reduction techniques in Wang *et al.* (2001) are used to change the elements of $C(s)$ into PID forms and yield the multivariable PID controller $\hat{C}(s)$.

The design procedure for MIMO systems is summarized as follows.

Step 1. Work out $D(s)$ for $G(s)$ to get $Q(S)$ and derive $\hat{Q}(s)$ if elements in $Q(s)$ are complicated with time-delay or irrational;

Step 2. Design k_{ii} for each $q_{ii}(s)$ or $\hat{q}_{ii}(s)$ using the Root-locus or Nyquist plot method;

Step 3. Construct $C(s)$ with k_{ii} and derive $\hat{C}(s)$ based on $C(s)$.

We now provide examples to illustrate the design procedure in detail.

Example 4.6. Consider a multivariable process,

$$G(s) = \begin{bmatrix} \frac{1}{s+1} & \frac{1}{s+2} \\ \frac{1}{s+3} & \frac{1}{s+1.5} \end{bmatrix}.$$

By choosing $d_{11}(s) = d_{22}(s) = 1$, the decoupler is designed as

$$D(s) = \begin{bmatrix} 1 & -\frac{s+1}{s+2} \\ -\frac{s+1.5}{s+3} & 1 \end{bmatrix},$$

according to (4.11), so we have

$$Q(s) = \begin{bmatrix} \frac{2.5s+4.5}{(s+1)(s+2)(s+3)} & 0 \\ 0 & \frac{2.5s+4.5}{(s+1.5)(s+2)(s+3)} \end{bmatrix}.$$

There is no need to derive $\hat{Q}_(s)$ since elements in $Q(s)$ are delay free and rational.

For $q_{22}(s)$, if the desired damping ratio is $\xi = 0.6$ and the desired 2%-settling time is $T_s = 7.13$, the dominant poles are $p_{1,2} = 0.5610 \pm 0.7480j$. We take $m = 3$ and use the Root-locus method. $K_{P11} = 1$ is chosen. The PID controller is obtained as

$$k_{11}(s) = 1 + \frac{1.5595}{s} + 0.5159s.$$

For $q_{22}(s)$, if the desired damping ratio is $\xi = 0.6$ and the desired 2%-settling time is $T_s = 7.13$, the dominant poles are $p_{1,2} = 0.5610 \pm 0.7480j$. We also take $m = 3$ and use the Root-locus method. $K_{P22} = 1$ is chosen. The PID controller is obtained as

$$k_{22}(s) = 1 + \frac{2.0703}{s} + 0.9231s.$$

$C(s)$ is calculated according to (4.12),

$$\begin{aligned} C(s) &= \begin{bmatrix} k_{11}(s)d_{11}(s) & k_{22}(s)d_{12}(s) \\ k_{11}(s)d_{21}(s) & k_{22}(s)d_{22}(s) \end{bmatrix} \\ &= \begin{bmatrix} 1 + \frac{1.5595}{s} + 0.5159s & -\frac{s+1}{s+2}\left(1 + \frac{2.0703}{s} + 0.9231s\right) \\ -\frac{s+1.5}{s+3}\left(1 + \frac{1.5595}{s} + 0.5159s\right) & 1 + \frac{2.0703}{s} + 0.9231s \end{bmatrix}. \end{aligned}$$

Both $c_{12}(s)$ and $c_{21}(s)$ resulted are high-order controllers. Using the method in Wang *et al.* (2001), their PID-type estimates are obtained and we have

$$\hat{C}(s) = \begin{bmatrix} 1 + \frac{1.5595}{s} + 0.5159s & -1.0029 - \frac{1.0352}{s} - 0.4668s \\ -0.7562 - \frac{0.7798}{s} - 0.3404s & 1 + \frac{2.0703}{s} + 0.9231s \end{bmatrix}.$$

The multivariable PID control system is constructed using $\hat{C}(s)$. The step responses of the resultant multivariable PID control system are shown in Figure 4.10, in solid lines. Step responses of the control system using the high-order controller $C(s)$ are also given in dashed lines for comparison. The performance is satisfactory.

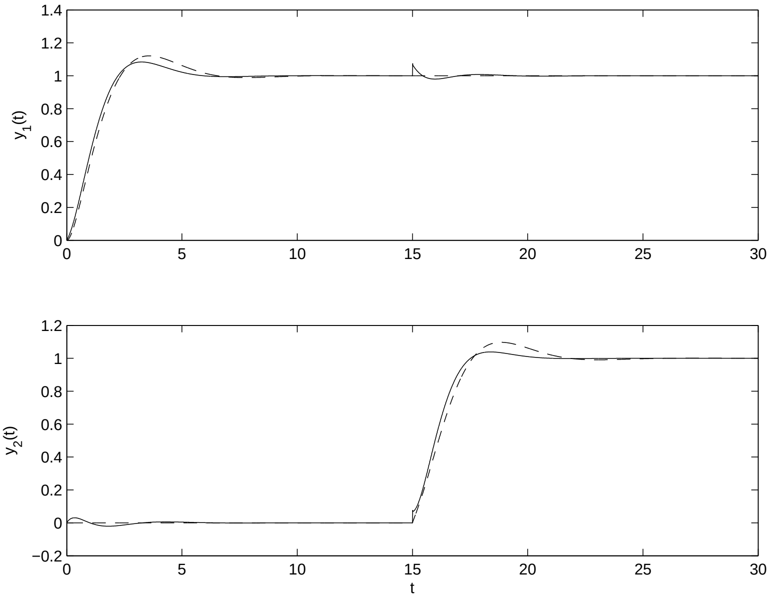

Figure 4.10. Step Response for Example 4.6 (Solid line, $\hat{C}(s)$; dashed line, $C(s)$)

Example 4.7. Consider the Vinate and luyben plant,

$$G(s) = \begin{bmatrix} \frac{-0.2e^{-s}}{7s+1} & \frac{1.3e^{-0.3s}}{7s+1} \\ \frac{-2.8e^{-1.8s}}{9.5s+1} & \frac{4.3e^{-0.35s}}{9.2s+1} \end{bmatrix}.$$

By choosing $d_{11}(s) = 1$ and $d_{22}(s) = e^{-0.7s}$, the decoupler is designed as

$$D(s) = \begin{bmatrix} 1 & 6.5 \\ \frac{2.8(9.2s+1)e^{-1.45s}}{4.3(9.5s+1)} & e^{-0.7s} \end{bmatrix},$$

according to (4.11). We have,

$$\begin{aligned} Q(s) &= G(s)D(s) \\ &= \begin{bmatrix} \frac{-0.2e^{-s}}{7s+1} + \frac{3.64(9.2s+1)e^{-1.75s}}{4.3(9.5s+1)(7s+1)} & 0 \\ 0 & \frac{-7.84e^{-1.8s}}{9.5s+1} + \frac{4.3e^{-1.05s}}{9.2s+1} \end{bmatrix}. \end{aligned}$$

The first-order time-delay model $\hat{Q}(s)$ is obtained by using the method proposed in Wang *et al.* (2001),

$$\hat{Q}(s) = \begin{bmatrix} \frac{0.08677e^{-1.86s}}{s+0.1342} & 0 \\ 0 & \frac{-1.459e^{-2.27s}}{s+0.105} \end{bmatrix}.$$

For $\hat{q}_{11}(s)$, if the desired damping ratio is $\xi = 0.7$ and the desired 2%-settling time $T_s = 47.48$, the dominant poles are $p_{1,2} = -0.0842 \pm 0.0859j$. We take $m = 3$ and use the Nyquist plot method. $K_{P11} = 0.85$ is chosen and the PID controller is obtained as

$$k_{11}(s) = 0.8500 + \frac{0.1803}{s} + 1.8096s.$$

For $\hat{q}_{22}(s)$, if the desired damping ratio is $\xi = 0.7$ and the desired 2%-settling time $T_s = 60.00$, the dominant poles are $p_{1,2} = -0.0668 \pm -0.0681j$. We also take $m = 3$ and use the Nyquist plot method. $K_{P22} = -0.04$ is chosen and the PID controller is obtained as

$$k_{22}(s) = -0.0400 - \frac{0.0067}{s} - 0.1031s.$$

$C(s)$ is calculated according to (4.12),

$$\begin{aligned} C(s) &= \begin{bmatrix} k_{11}(s)d_{11}(s) & k_{22}(s)d_{12}(s) \\ k_{11}(s)d_{21}(s) & k_{22}(s)d_{22}(s) \end{bmatrix} \\ &= \begin{bmatrix} 0.8500 + \frac{0.1803}{s} + 1.8096s & 6.5\left(-0.0400 - \frac{0.0067}{s} - 0.1031s\right) \\ \frac{2.8(9.2s+1)e^{-1.45s}}{4.3(9.5s+1)}\left(0.8500 + \frac{0.1803}{s} + 1.8096s\right) & e^{-0.7s}\left(-0.0400 - \frac{0.0067}{s} - 0.1031s\right) \end{bmatrix}. \end{aligned}$$

Both $c_{21}(s)$ and $c_{22}(s)$ resulted are high-order controllers. Using the method in Wang *et al.* (2001), their PID-type estimates are obtained and we have

$$\hat{C}(s) = \begin{bmatrix} 0.8500 + \frac{0.1803}{s} + 1.8096s & -0.2600 - \frac{0.0435}{s} - 0.6701s \\ 0.5197 + \frac{0.1174}{s} + 1.3221s & -0.0354 - \frac{0.0067}{s} - 0.0767s \end{bmatrix}.$$

The multivariable PID control system is constructed using $\hat{C}(s)$. The step responses of the resultant multivariable PID control system are shown in Figure 4.11, in solid lines. Step responses of the control system using the high-order controller $C(s)$ are also given in dashed lines for comparison. The performance is satisfactory.

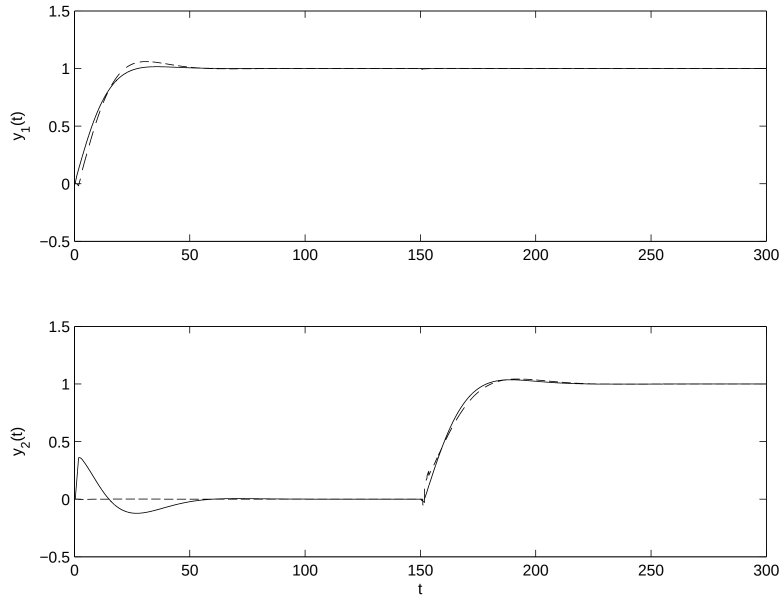

Figure 4.11. Step Response for Example 4.7 (Solid line, $\hat{C}(s)$; dash line, $C(s)$)

Example 4.8. Consider the well-known Wood/Berry process,

$$G(s) = \begin{bmatrix} \frac{12.8e^{-s}}{16.7s+1} & \frac{-18.9e^{-3s}}{21.0s+1} \\ \frac{6.6e^{-7s}}{10.9s+1} & \frac{-19.4e^{-3s}}{14.4.5s+1} \end{bmatrix}.$$

By choosing $d_{11}(s) = d_{22}(s) = 1$, the decoupler is designed as

$$D(s) = \begin{bmatrix} 1 & \frac{(315.63s+18.90)e^{-2s}}{268.80s+12.80} \\ \frac{(95.04s+6.60)e^{-4s}}{211.46s+19.40} & 1 \end{bmatrix},$$

according to (4.11). We have,

$$\begin{aligned} Q(s) &= G(s)D(s) \\ &= \begin{bmatrix} \frac{12.8e^{-s}}{16.7s+1} + \frac{-18.9e^{-3s}}{21.0s+1} \cdot \frac{(95.04s+6.60)e^{-4s}}{211.46s+19.40} & 0 \\ 0 & \frac{6.6e^{-7s}}{10.9s+1} \cdot \frac{(315.63s+18.90)e^{-2s}}{268.80s+12.80} + \frac{-19.4e^{-3s}}{14.4.5s+1} \end{bmatrix}. \end{aligned}$$

The first-order time-delay model $\hat{Q}(s)$ is obtained as,

$$\hat{Q}(s) = \begin{bmatrix} \frac{6.374e^{-1.065s}}{5.414s+1} & 0 \\ 0 & \frac{-9.691e^{-3.12s}}{7.942s+1} \end{bmatrix}.$$

For $\hat{q}_{11}(s)$, if the desired damping ratio is $\xi = 0.7$ and the desired 2%-settling time $T_s = 32.35$, the dominant poles are $p_{1,2} = -0.1236 \pm 0.1261j$. We take $m = 3$

and use the Nyquist plot method. $K_{P11} = 0.2$ is chosen and the PID controller is obtained as

$$k_{11}(s) = 0.200 + \frac{0.0416}{s} + 0.5470s.$$

For $\hat{q}_{22}(s)$, if the desired damping ratio is $\xi = 0.7$ and the desired 2%-settling time $T_s = 59.14$, the dominant poles are $p_{1,2} = 0.0676 \pm 0.0690j$. We take $m = 3$ and use the Nyquist plot method. $K_{P22} = -0.08$ is chosen and the PID controller is obtained as

$$k_{22}(s) = -0.0800 - \frac{0.0110}{s} - 0.4143s.$$

$C(s)$ is calculated according to (4.12),

$$\begin{aligned} C(s) &= \begin{bmatrix} k_{11}(s)d_{11}(s) & k_{22}(s)d_{12}(s) \\ k_{11}(s)d_{21}(s) & k_{22}(s)d_{22}(s) \end{bmatrix} \\ &= \begin{bmatrix} 0.2 + \frac{0.0416}{s} + 0.547s & \frac{(315.63s+18.9)e^{-2s}}{268.8s+12.8}\left(-0.08 - \frac{0.011}{s} - 0.4143s\right) \\ \frac{(95.04s+6.6)e^{-4s}}{211.46s+19.4}\left(0.2 + \frac{0.0416}{s} + 0.547s\right) & -0.08 - \frac{0.011}{s} - 0.4143s \end{bmatrix}. \end{aligned}$$

Both $c_{12}(s)$ and $c_{21}(s)$ resulted are high-order controllers. Using the method in Wang *et al.* (2001), their PID-type estimates are obtained and we have

$$\hat{C}(s) = \begin{bmatrix} 0.2000 + \frac{0.0416}{s} + 0.5470s & -0.0682 - \frac{0.0162}{s} - 0.3707s \\ 0.1103 + \frac{0.0142}{s} - 0.0200s & -0.0800 - \frac{0.0110}{s} - 0.4143s \end{bmatrix}.$$

The multivariable PID control system is constructed using $\hat{C}(s)$. The step responses of the resultant multivariable PID control system are shown in Figure 4.12, in solid lines. Step responses of the control system using the high-order controller $C(s)$ are also given in dashed lines for comparison. The performance is satisfactory.

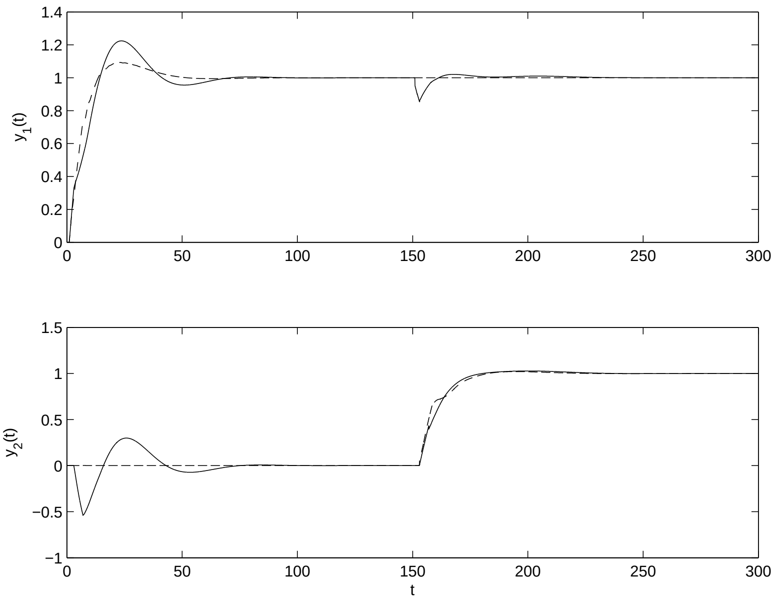

Figure 4.12. Step Response for Example 4.8 (Solid line, $\hat{C}(s)$; dash line, $C(s)$)

4.6 Conclusion

Two simple yet effective methods have been presented for guaranteed dominant pole placement by PID, based on Root locus and Nyquist plot respectively. Each method is demonstrated with examples. The extension to MIMO systems is also provided. Obviously, the methods are not limited to PID controllers. They can be extended to other controllers where one controller parameter is used as the variable gain and all other parameters are solved in terms of this gain to meet the fixed pole requirements.

Chapter 5

Internet-based Control Systems Design with PID Controllers

5.1 Introduction

As has been discussed in Chapter 1, internet-based control systems use the internet for remote control and monitoring of plants. They are easy-to-access and not limited to any geographical location. Internet-based control systems have found their applications in many areas, such as telerobots, manufacturing industry, and virtual laboratories(Yang, 2006; Srivastava and Kim, 2003; Sung *et al.*, 2001; Overstreet and Tzes, 1999; Yang and Alty, 2002). In 2001 Oboe developed a telerobotics system which allows the internet users to command a robot in real time with both visual and force feedback(Oboe, 2001). At Integrated Manufacturing Lab of UC Berkeley, a World-Wide-Web design to fabrication tool called Cybercut was developed. To facilitate engineering education, many universities have started virtual laboratories for their students to perform experiments outside campus. As the internet technology develops and matures, internet-based control systems are expected to be more popular in the future.

Many researchers have been working on internet-based control systems during the past few years. Because random time delays caused by the internet undermine the stability of the closed-loop control systems, intensive research was done on stability analysis and methods to tackle instability and uncertainty. Many control methodologies were proposed in the literature(Tipsuwan and Chow, 2003; Guan and Yang, 2006). However, due to the difficult nature of this problem, few encouraging and simple result has found so far. Adopting a different approach to solve the stability issue is necessary.

Research has also been done on how the sampling time selection affects the control performance (Yu *et al.*, 2004; Lian *et al.*, 2002). It is found that when the sampling time becomes smaller in a distributed networked control system, although the performance improves in the beginning, it deteriorates eventually. That is because a small sampling time also means a heavy load on the network and the heavy load would cause long time delays or data transfer failures. Nevertheless, nobody has worked out how the control performance is affected by the sampling time. In other words, the question about what values the sampling time should take given a specific requirement on the control performance remans open.

Furthermore, although most of the design methods proposed so far ensure system stability, they are unable to meet certain requirements on control performance, such as overshoot and settling time of step response. To meet the control performance requirements is constrained by the limit of load on the internet. The load on the internet, represented by the sampling time of the control system, should be kept as small as possible. Therefore, there is a need to work out a way which meets the control performance requirements subject to load minimization on the internet.

This chapter proposes such a load minimization design method for the internet-based control systems with dynamic performance specifications. It resolves the stability problems with a dual-rate configuration. As illustrated in Figure 1, the dual-rate control system (Yang and Yang, 2007) is a two-level control architecture, the lower level of which guarantees that the plant is under control even when the network communication is lost for a long time. The higher level of the control architecture implements the global control function. The two levels run at different sampling times. The lower level runs at a small sampling time (higher frequency) to stabilize the plant, while the higher level at a big sampling time (lower frequency) to reduce the communication load and increase the possibility of receiving data on time. With the local system stable and the inputs of the remote controller bounded, the overall control system would remain stable. The PID controller is used for the remote control loop for simplicity and ease of tuning. The requirements on control performances, such as overshoot and settling time of step response, are represented a pair of conjugate poles. With the dominant pole placement method we work out the upper bounds of the remote control system's sampling time and design the remote PID controller. The novelty of this method is focused on guaranteeing both control performance and stability of Internet-based control systems and minimizing the data transmission load over the Internet simultaneously by maximizing the remote controller sampling time.

5.2 Problem Formulation

Consider an internet-based control system as shown in Figure 5.1. It is a discrete-time control system by nature. The dual-rate scheme is used here, which basically means the local control loop has a smaller sampling time than the remote loop. The local controller stabilizes the plant and also meets the performance requirements on the local control system. The PID controller, located over the other side of the internet, remotely regulates the output according to the desired reference. The control input from the remote controller comes to the local control system via the internet. The feedback signal from the local control system is sent to the remote controller by the internet.

The transmission vis the internet brings time delay inevitably. Suppose the time delay of feedback via the internet is T_b and time delay of feedforward is T_f. We can replace the internet block with two blocks of time delays, e^{-T_b} and e^{-T_f}. Both T_b and T_f are random variables, which is considered as the prime cause of instability and difficulty in control. However, in reality, the ranges of the time

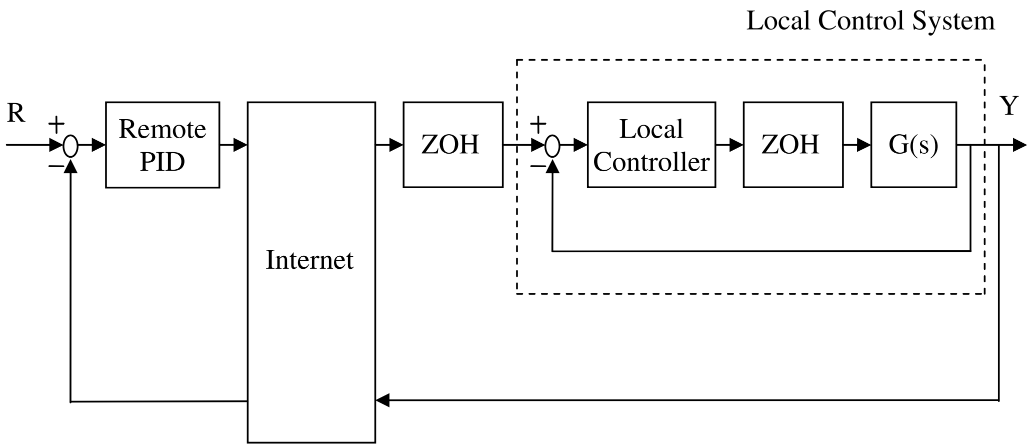

Figure 5.1. Control scheme

delays are approximately known. It means

$$0 < T_b \leq \overline{T}_b, 0 < T_f \leq \overline{T}_f.$$

where, $\overline{T}_b$ and $\overline{T}_f$ are upper bounds for the time delay of feedback and feedforward respectively.

To access the performance of a discrete-time system is difficult since there is no handy formula or method which could be used. We need to transform the original discrete-time system into continuous-time through some approximations so that the second-order model and dominant pole placement method can be used.

Denote the sampling time of the local loop by T_l and that of the remote loop by T_r. Approximate the Zero-Order-Hold as a time delay of half the sampling time, and transform the internet-based control system into a conventional continuous-time system. The two ZOHs shown in Figure 5.1 are essentially another two blocks of time delays, $e^{-0.5T_l}$ and $e^{-0.5T_r}$. For the sake of simplicity, the continuous-time block diagram, is redrawn in Figure 5.2.

The remote sampling time is used as a measurement of load on the internet. Load minimization for the internet is to maximize the remote sampling time. The overshoot and settling time of step response are chosen as the index of dynamic performance. Our problem at hand is to design the local controller and remote

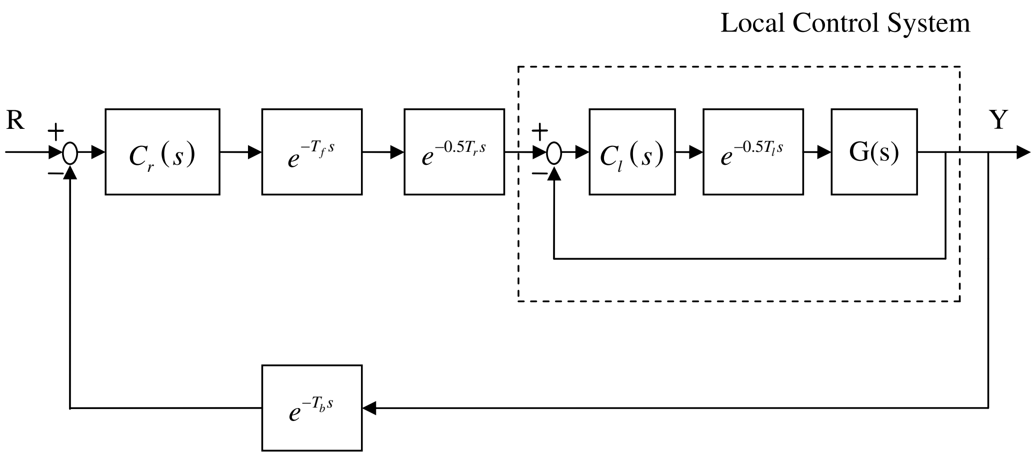

Figure 5.2. Block diagram

PID controller so as to minimize the load on the internet subject to these dynamic performance specifications.

5.3 Proposed Method

As the type of controller to use for a given plant in the local control system is not limited and a fast sampling time is possible, there are many methods to design the local controller. Throughout this paper, the plant would not be studied directly for simplicity. It is assumed that the local control system is already stable and fulfills the control specifications. The model of the local control system can be obtained from the step response method, or model reduction methods like the one presented in Liu *et al.* (2007). Thereby, we have a new and simpler block diagram as shown in Figure 5.3, in which $G_l(s)$ is the transfer function of the local control system.

From the dead time, overshoot and settling time of the step response, the local system is modelled as first or second order with time delay. If the step response of $G_l(s)$ has certain overshoot, it is approximated as a second-order transfer function:

$$G_l(s) = \frac{1}{as^2 + bs + c} e^{-sL}.$$

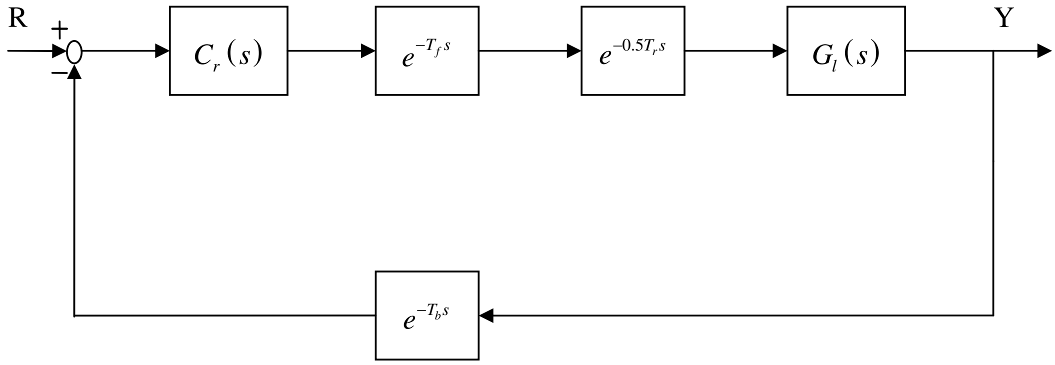

Figure 5.3. Simplified block diagram

If there is no overshoot, it would be approximated as first-order:

$$G_l(s) = \frac{1}{Ts+1}e^{-sL}.$$

We use the method presented in Wang *et al.* (1999) in tuning of the remote PID or PI controller. The reason is that it cancels out the denominator of $G_l(s)$ with the nominator of $C_r(s)$ and transfers our problem to a simple one-variable one. Write the transfer function of $C_r(s)$ as

$$C_r(s) = k\frac{as^2+bs+c}{s}, \tag{5.1}$$

if $G_l(s)$ is second-order, or

$$C_r(s) = k\frac{Ts+1}{s}, \tag{5.2}$$

if $G_l(s)$ is first-order. In both cases the open-loop transfer function becomes

$$Q(s) = G_l(s)C_r(s)e^{-\left(T_f+T_b+0.5T_r\right)s} = \frac{k}{s}e^{-\left(T_f+T_b+L+0.5T_r\right)s}.$$

The only variable left to determine for the controller is k. k affects both the stability and performance of the closed-loop system.

Firstly it is necessary to study the stability of the overall closed-loop transfer function with respect to k. An equivalent case is found when a pure integral process with time delay is controlled by a simple P controller. That has been studied in

(Lu, 2006) and the range of k is found to be

$$0 < k < \frac{\pi}{2\left(T_f + T_b + L + 0.5T_r\right)}. \tag{5.3}$$

We use the method of dominant pole placement to find a suitable k. Suppose the requirements on the overshoot and settling time of step response are represented by a pair of the poles, $p_{1,2} = -\omega\zeta \pm j\omega\sqrt{1-\zeta^2}$, where ζ is the closed-loop damping ratio. Substituting them into the closed-loop characteristic equation

$$1 + Q(p_1) = 0$$

gives

$$k = \omega e^{-\omega\zeta\left(T_f + T_b + L + 0.5T_r\right)}, \tag{5.4}$$

where

$$\omega = \frac{cos^{-1}\zeta}{\sqrt{1-\zeta^2}\left(T_f + T_b + L + 0.5T_r\right)}.$$

Suppose these two poles, $p_{1,2} = -\omega\zeta \pm j\omega\sqrt{1-\zeta^2}$, are dominant, the settling time of step response is roughly (Astrom and Hagglund, 1995),

$$t_s \approx \frac{4}{\omega\zeta} + \left(T_f + L + 0.5T_r\right).$$

With the value of ω in (5.4) the above equation becomes,

$$t_s \approx \frac{4\sqrt{1-\zeta^2}\left(T_f + T_b + L + 0.5T_r\right)}{\zeta cos^{-1}\zeta} + \left(T_f + L + 0.5T_r\right).$$

Given a performance requirement on settling time,

$$t_s \leq \bar{t}_s,$$

the range of T_r should be

$$T_r \leq \frac{\bar{t}_s - \frac{4\sqrt{1-\zeta^2}}{\zeta cos^{-1}\zeta}\left(T_b + T_f + L\right) - T_f - L}{\frac{2\sqrt{1-\zeta^2}}{\zeta cos^{-1}\zeta} + 0.5}. \tag{5.5}$$

Because T_f and T_b are random with certain ranges and it is impossible to find the exact value, the most conservative upper bounds are chosen to recalculate the stabilizing range of k ensuring stability, so (5.3) becomes

$$0 < k < \frac{\pi}{2\left(\overline{T}_f + \overline{T}_b + L + 0.5T_r\right)}. \tag{5.6}$$

Applying the upper bounds of T_f and T_b into (5.4) gives

$$k = \omega e^{-\omega\zeta\left(\overline{T}_f+\overline{T}_b+L+0.5T_r\right)}, \tag{5.7}$$

where

$$\omega = \frac{cos^{-1}\zeta}{\sqrt{1-\zeta^2}\left(\overline{T}_f+\overline{T}_b+L+0.5T_r\right)}.$$

And (5.5) becomes

$$T_r \leq \frac{\bar{t}_s - \frac{4\sqrt{1-\zeta^2}}{\zeta cos^{-1}\zeta}\left(\overline{T}_b+\overline{T}_f+L\right) - \overline{T}_f - L}{\frac{2\sqrt{1-\zeta^2}}{\zeta cos^{-1}\zeta}+0.5}. \tag{5.8}$$

Experiences show satisfactory responses are obtained if closed-loop poles of damping ratio $\zeta = 0.7071$ are chosen. By (5.8) the range of T_r becomes

$$T_r \leq \frac{\bar{t}_s - 6.1L - 5.1\overline{T}_b - 6.1\overline{T}_f}{3.05}. \tag{5.9}$$

And substituting $\zeta = 0.7071$ into (5.7) yields

$$k = \frac{0.5}{\overline{T}_f+\overline{T}_b+L+0.5T_r}. \tag{5.10}$$

Since this value is within the range provided by (5.6), the resulted system is stable. The largest allowable T_r based on (5.9) is taken to calculate k in (5.10) and design the remote PID controller.

5.4 Simulation Example

Let us look at an example and demonstrate the use of our proposed method.

Example 5.1. Consider the local system $G_l(s)$ and use the step response method to determine its transfer function. It has a step response with a dead time 2 seconds, overshoot 10% and settling time 7 s. The transfer function is approximated

$$G_l(s) = \frac{1}{0.546s^2+0.8737s+1}e^{-2s}.$$

Suppose the largest possible time delay caused by the internet is 1 second,which means $\overline{T}_b = \overline{T}_f = 1$.

By (5.1) the remote PID controller is

$$C_r(s) = k\frac{0.546s^2 + 0.8737s + 1}{s}.$$

The next step to determine k according to the largest allowable settling time. If the largest allowable settling time is 30 second, according to (5.9) the range of the sampling time should be

$$T_r \leq 2.23.$$

When the sampling time is taken to be 2.23 seconds and k is calculated based on (5.10),

$$k = 0.0978.$$

so the controller is designed as

$$C_r(s) = \frac{0.0534s^2 + 0.0854s + 0.0978}{s}.$$

The step response is shown in Figure 5.4. The obtained settling time is 30.25 seconds and the response is satisfactory.

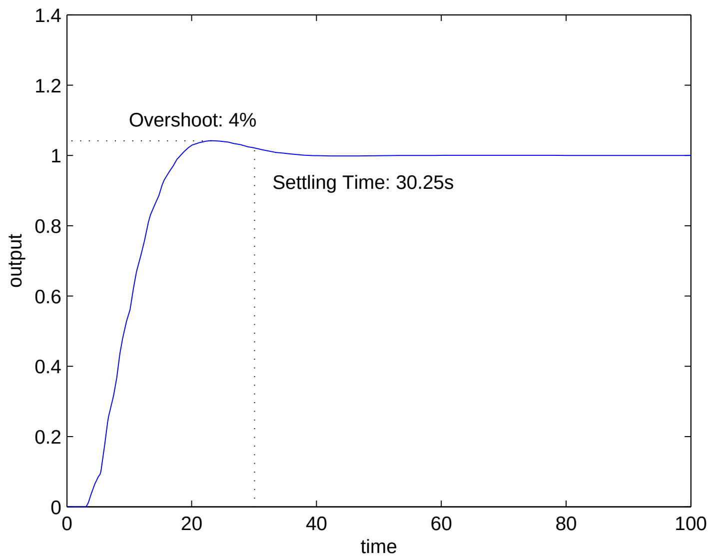

Figure 5.4. Step response in Example 5.1

5.5 Real-Time Implementation

In order to show the applicability and effectiveness of the proposed method, read-time experiments have been carried out in lab. The test was conducted on a real-time Process Control Unit (PCU) in the Network and Control Laboratory at Loughborough University, UK. Figure 5.5 shows the layout of the experimental system, which includes the PCU and the remote control system. Inside the PCU, there are the local control system and a water tank rig. The water tank rig consists of a process tank, sump, pump, cooler and several drain valves. Based on the measurements of the liquid level of the water tank and flow rate of the pump, the objective is to control the liquid level or flow rate of the water tank by regulating the flow rate of the pump. The local controller parameters and sampling interval are chosen by the local operator through an operation interface. The remote control system is connected to the PCU via the internet. More details on this experimental system can be found in Yang and Yang (2007). We have conducted two experiments separately, one on flow rate control and the other on liquid level control.

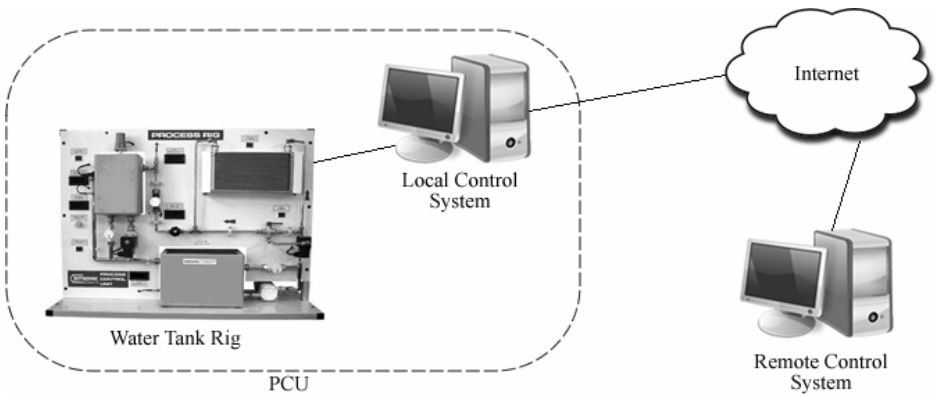

Figure 5.5. Experimental system layout

Flow Rate Control: The first step is get the model of the local control system using the step response method. A step change in the setpoint of the flow rate has been introduced into the local flow rate control system. The step response is with 14.9% overshoot and 9.9 seconds settling time. The dead time is 0.5 second in average. Therefore, the local close-loop control system is modelled as a second-order object with a transfer function:

$$G_l(s) = \frac{1}{2.922s^2 + 1.771s + 1} e^{-0.5s}.$$

The largest possible time delay caused by the internet between the local and remote controllers is 0.5 second, which means

$$\overline{T}_b = \overline{T}_f = 0.5.$$

By (5.1) the remote PID controller is

$$C_r(s) = k\frac{2.922s^2 + 1.771s + 1}{s}.$$

If the largest allowable settling time is set as 15 seconds, when the dead time is $L = 0.5$, the range of the remote sampling time according to (5.9) should be

$$T_r \leq 2.082$$

When the remote sampling time is taken to be 2.082 seconds, the largest value in order to minimize the data transmission load, and k is calculated based on (5.10)

$$k = 0.197.$$

The remote flow rate controller is designed as

$$C_r(s) = 0.348 + \frac{0.197}{s} + 0.576s.$$

A step response of the remote controller has overshoot 12% and 11.4 seconds settling time as shown in Figure 5.6. The unit of the flow rate is liter per minute (L/min). The performance is satisfactory.

If the remote sampling time is taken to be 4 seconds, which is out of the range of $(0,\ 2.082]$, then k is calculated based on (5.10):

$$k = 0.143.$$

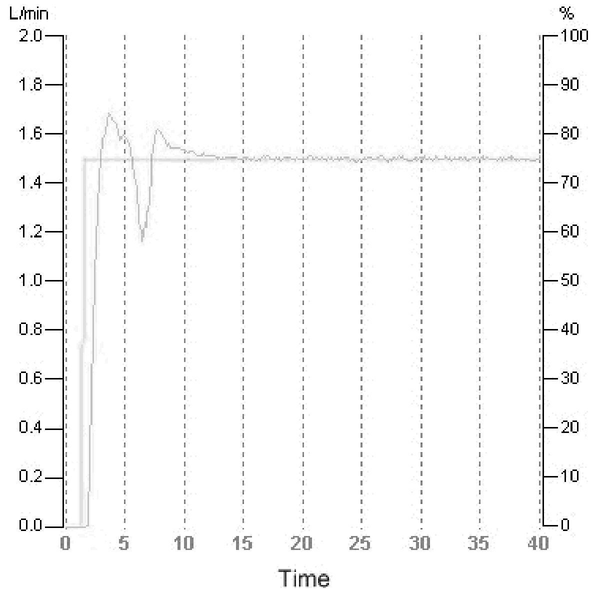

Figure 5.6. Step response of flow rate control when $T_r = 1s$

The remote flow rate controller is designed as

$$C_r(s) = 0.253 + \frac{0.143}{s} + 0.418s.$$

A step response of the remote controller has overshoot 14% and 15.2 seconds settling time as shown in Figure 5.7. The performance is unsatisfactory as the settling time is great than the desirable value 15 seconds.

Liquid Level Control: Similar experimental procedures have been carried out for the liquid level control in the PCU. A step change in the setpoint of the liquid level has been introduced into the local liquid level control system. The step response has no overshoot and the settling time is 28.6 seconds. The dead time L is 1.5 seconds in average. Since there is no overshoot, the local close-loop control system is modelled as a first-order object with a transfer function:

$$G_l(s) = \frac{1}{9.533s + 1} e^{-0.5s}.$$

The largest possible time delay caused by the Internet between the local and remote controllers is still kept at 0.5 second. It means

$$\overline{T}_b = \overline{T}_f = 0.5.$$

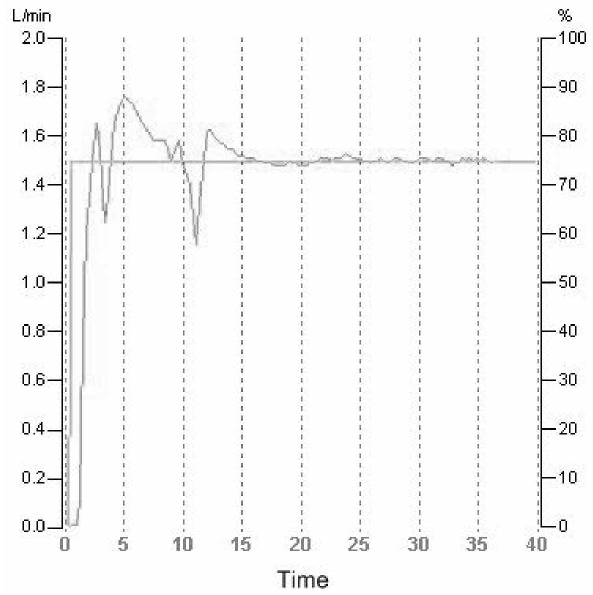

Figure 5.7. Step response of flow rate control when $T_r = 4s$

By (5.2) the remote PID controller is

$$C_r(s) = k\frac{9.533s + 1}{s}.$$

If the largest allowable settling time is set as 30 seconds, when the dead time $L = 1.5s$, the range of the sampling time according to (5.9) should be

$$T_r \leq 5.$$

When the remote sampling time is taken to be 5 seconds, the largest value, and k is calculated based on (5.10)

$$k = 0.1.$$

The remote liquid level controller is designed as

$$C_r(s) = 0.962 + \frac{0.1}{s}.$$

A step response of the remote controller has no overshoot and 29.5 seconds settling time as shown in Figure 5.8. The unit of the liquid level is %. The performance is satisfactory as the settling time is less than the desirable value 30 seconds.

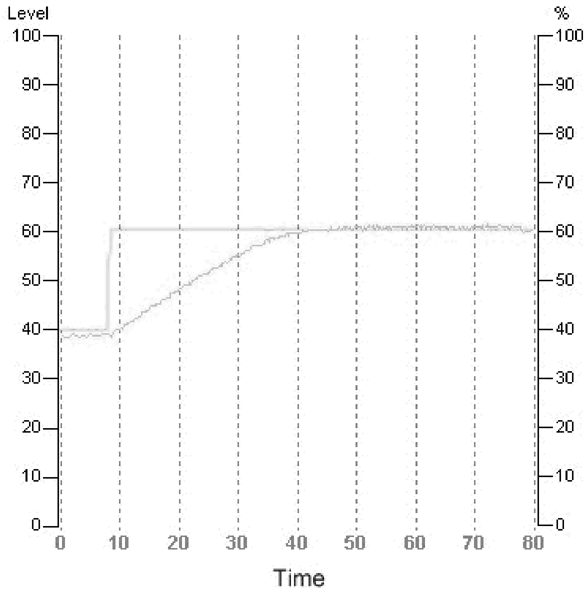

Figure 5.8. Step response of liquid level control when $T_r = 4s$

If the remote controller sampling time is taken to be 10 seconds, which is out of the range of $(0,\ 5]$, then k is calculated based on (5.10)

$$k = 0.067.$$

The remote liquid level controller is designed as

$$C_r(s) = 0.636 + \frac{0.067}{s}.$$

A step response of the remote controller has no overshoot and settling time 32.6s as shown in Figure 5.9. The performance is unsatisfactory as the settling time is great than the desirable value 30 seconds.

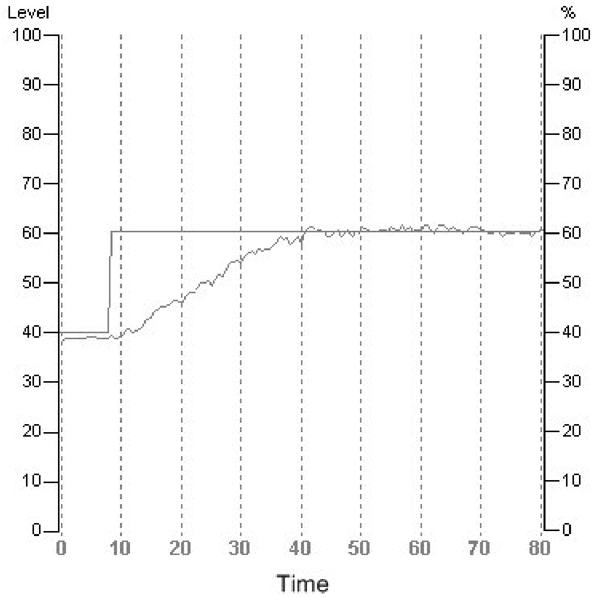

Figure 5.9. Step response of liquid level control when $T_r = 10s$

5.6 Conclusion

In this chapter a method to meet performance requirements and minimize load on the network for internet-based control systems is presented. The relationship between the sampling time and settling time of the system step response is worked out. The remote PID controller is tuned to fulfill the requirement on the settling time of step response and maximize the sampling time. Good responses in simulation examples and real-time implementation are obtained.

Chapter 6

Conclusion

6.1 Main Findings

PID control has been an active research area for more than half a century. Although an abundant amount of study has been done and many tuning methods have been proposed, there is still much room for improvement. In this thesis the following new results are found on PID controller systems.

A. Relationship on Stabilizability of LTI Systems by P and PI Controllers

The relationship on stabilizability of linear time-invariant (LTI) systems by P and PI controllers is investigated. It is found that PI can stabilize all the systems that P stabilizes but the converse is not true in general. It means PI is no poorer than P in stabilization. PI can stabilize all the systems P stabilizes but P cannot stabilize all the systems P stabilizes. The cases with the equivalence of stabilizability by P and PI are established and they are in general low-order systems with few zeros. The cases with non-equivalence are also identified and presented.

B. Simple Tuning Methods for PID Controllers

Firstly, a framework for PID controller design is presented which leads to the important popular setting, $T_i = 4T_d$. This setting first appeared in the Ziegler and Nichols tuning and has been widely adopted so far. The framework also provides some analytical PID tuning formulas with improved performance over the ZN tuning. Secondly, a simple PID tuning method for dominant poles and phase margin specification is proposed. Time domain specifications such as settling time and percentage overshoot are represented by a pair of dominant poles, which is combined with phase margin specification to achieve closed-loop stability and robustness. A graphical way is developed to determine PID settings to meet these specifications simultaneously.

C. Guaranteed Dominant Pole Placement with PID Controllers

Guaranteed dominant pole placement with PID controllers is achieved with two simple and easy methods. They are based on Root-Locus and Nyquist plot respectively. In the Root-Locus method the roots of the closed-loop characteristic equation for all the positive values of K_P are plotted and the range of K_P such that the roots other than the chosen dominant pair are all in the desired region is then determined. In the Nyquist plot method the same idea is used but the Nyquist contour is modified. If a solution exists, the parametrization of all the solutions is explicitly given. The extension of these two methods to MIMO systems is also discussed. Together with the model reduction techniques, the multivariable PID controller is developed. Satisfactory performances are obtained in the examples.

D. Internet-based Control Systems Design with PID Controllers

A new design method for internet-based control systems in a the dual-rate configuration to achieve load minimization and dynamic performance specifications is proposed. It avoids the complexity of large scale system design by focusing on individual control systems. In the dual-rate configuration, the plant under control is first stabilized by a local controller with a high sampling rate. The remote PID controller, which regulates the output according to the desirable reference, adopts a low sampling rate to reduce load on the network. The upper bound of the remote PID controller's sampling time which meets the requirement on control performance is derived and a simple tuning method for the remote PID controller is presented.

6.2 Suggestions for Further Work

The thesis has taken the full route from initial ideas, via theoretical developments, to methodologies that can be applied to relevant engineering problems. Several new results have been obtained but some topics remain open and are recommended for future work.

A. Relationship on Stabilizability of LTI Systems with Time-Delay by P and PI Controllers

Relationship on stabilizability of LTI systems by P and PI controllers are discussed in this thesis. The discussion includes all delay-free plants and time-delay plants of first or second order, but the time-delay plants of higher order are left out due to the time constraint. Nevertheless, it is meaningful and worthwhile to study stabilizability of these plants by P and PI controllers, although several difficulties are expected. To choose an effective analysis tool is one of the difficulties. When the time-delay plants are of high order, their Nyquist plots are complicated but can still used in the analysis. It may be related to the case by P and PI, but might not be identical since a general PID may not be written as a PD cascaded with PI one.

B. Simple Tuning Methods for PID Controllers

In the tuning method for dominant poles and phase margin, a graphical way is used to find out the parameters of the PID controller. Two figures are plotted to find out K_I and the other two parameters are determined based on that. In practice, figures plotting might be time-consuming and troublesome. Some other simple ways to determine the parameters for the design can improve the proposed method.

C. Guaranteed Dominant Pole Placement with PID Controllers for MIMO Systems

The proposed guaranteed dominant pole placement with PID controllers is mainly focused on SISO systems. Extension to MIMO systems of guaranteed dominant pole placement with PID controllers is provided but the procedures are not so simple or effective. The model reduction techniques are used several times and the poles might have changed in the end, although the performance does not deteriorate much as demonstrated by the examples. Another effective and simple method is needed to guarantee the assigned poles and solve this problem.

D. MIMO Internet-based Control Systems Design with PID Controllers

In this thesis, internet-based control systems design with PID controllers is provided for SISO systems. The design, like the guaranteed dominant pole placement, can also be extended to MIMO systems. For MIMO systems, the proposed method may encounter problems, such as coupling and different time delays of elements in the systems. One possible solution is to make the system decoupled and then apply the proposed methods to each element in the decoupled loop.

Bibliography

Ang, K. H., G. Chong and Y. Li (2005). PID control system analysis, design and technology. *IEEE Transaction on Control Systems Technology* **13**(4), 559.

Astrom, K. J. and T. Hagglund (1984). Automatic tuning of simple regulators with specifications on phase and amplitude margins. *Automatica* **20**(5), 645–651.

Astrom, K. J. and T. Hagglund (1995). *PID controller: Theory, Design and Tuning, second edition*. Instrument Society of America. Research Triangle Park, NC.

Cohen, G. H. and G. A. Coon (1953). Theoretical consideration of retarded control. *Trans. ASME* **75**, 827–834.

Fung, H. W., Q. G. Wang and T. H. Lee (1998). PI tuning in terms of gain and phase margins. *Automatica* **34**(9), 1145–1149.

Gu, K., V. Kharitonov and J. Chen (2003). *Stability of Time-delay Systems*. Birkhauser. Boston.

Guan, Z. H. and S. H. Yang (2006). Stability of internet-based control systems with time-delay at feedback and feed-forward channels. *Proceedings of the 2006 IEEE International Conference on Network, Sensing and Control* pp. 649–653.

Ho, B. and T. F. Edgar (2004). PID control performance assessment: the single-loop case. *AIChE Journal* **50**(6), 1211–1218.

Ho, W. K., O. P. Gan, E. B. Tay and E. L. Ang (1996). Performance and gain and phase margins of well-known PID tuning formulas. *IEEE Transactions on Control System Technology* **4**(4), 473–477.

Hokayem, P.F. and C.T. Abdallah (2004). Inherent issues in networked control systems: a survey. *Proceeding of the 2004 American Control Conference, Boston, Massachesetts June 30 - July 2, 2004* pp. 4897–4902.

K., Ho. W., C. C. Hang and J. Zhou (1997). Self-tuning PID controller of a plant with under-damped response with specifications on gain and phase margins. *IEEE Transactions on Control System Technology* **5**(4), 446–452.

Lee, J. H. (2005). a new phase-lead design method using the root locus diagrams. *IEEE Transaction on Automatic Control* **50**(11), 1887–1891.

Lian, F. L., J. Moyne and D. Tilbury (2002). Network design consideration for distributed control systems. *IEEE Transactions on Control Systems Technology* **10**(2), 297–307.

Liu, M., Q. G. Wang, B. Huang and C. C. Hang (2007). Improved identification of continuous-time delay processes from piecewise step tests. *Journal of Process Control* **17**, 51–57.

Lu, X. (2006). *New Design for Control Systems*. National University of Singapore. Singapore.

Oboe, R. (2001). Web-interfaced, force-reflecting teleoperation systems. *IEEE Transactions on Industrial Electronics* **48**, 1257–1265.

Ogata, K. (2002). *Mordern Control Engineering, 4nd Edition*. Prentice Hall Inc.. Upper Saddle River, NJ.

Overstreet, J. W. and A. Tzes (1999). An internet-based real-time control engineering laboratory. *IEEE Control Systems Magnize* **19**(5), 19–34.

Persson, P. and K. J. Astrom (1993). Dominant pole design - a unified view of PID controller tuning. *Adaptive systems in control and signal processing 1992: selected papers from the Fourth IFAC Symposium, Grenoble, France, 1-3 July 1992* pp. 377–382.

Shen, J. C. (2001). Fuzzy neural networks for tuning controller for plants with underdamped responses. *IEEE Transaction on Fuzzy Systems* **9**(2), 333–342.

Srivastava, A. and W. J. Kim (2003). Internet-based supervisory control and stability analysis for time delay. *Proceedings of the 2003 American Control conference, Denver, Colorado* pp. 627–632.

Sung, H., V. Sundararajan, C. Smith, B. Kannan, R. Dsouza, G. Sun, A. Mohole, P. K. Wright, J. Kim, S. McMains, J. Smith and C. H. Sequin (2001). Cybercut: An internet-based cad/cam system. *Journal of Computing and Information Science in Engineering* **1**(1), 52–59.

Tang, W., S. J. Shi and M. X. Wang (2002). Autotuning PID control for large time-delay processes and its application to paper basis weight control. *Industr. and Eng. Chem. Res.* **41**, 4318–4327.

Tipsuwan, Y. and M.-Y. Chow (2003). Control methodologies in networked control systems. *Control Engineering Practice* **11**(10), 1099–1111.

Wang, Q. G. (2003). *Decoupling Control*. Springer-Verlag. Berlin-Heidelberg, Germany.

Wang, Q. G. and Y. Zhang (2001). Robust identification of continuous systems with dead-time from step responses. *Automatica* **37**, 377–390.

Wang, Q. G., C. C. Hang and X. P. Yang (2001). Single-loop controller design via IMC principles. *Automatica* **37**, 2041–2048.

Wang, Q. G., H. W. Fung and Y. Zhang (1999). PID tuning with exact gain and phase margins. *ISA Transactions* **38**, 243–249.

Yang, L and S. H. Yang (2007). Multi-rate control in internet-based control systems. *IEEE Transactions on Systems, Man and Cybernetics - Part C: Applications and Reviews* **37**(2), 185–192.

Yang, S. H. and J.L. Alty (2002). Development of a distributed simulator for control experiments through the internet. *Future Generation of Computer Systems* **18**(5), 595–611.

Yang, T. C. (2006). Networked control system: a brief survey. *IEE Proceedings Control Theory and Applications* **153**(4), 403–412.

Yu, J. Y., S. M. Yu and H. Q. Wang (2004). Survey on the performance analysis of networked control systems. *2004 IEEE International Conference on Systems, Man and Cybernetics* pp. 5068–5073.

Ziegler, J. G. and N. B. Nichols (1942). Optimum settings for automatic controllers. *Trans. ASME* **64**, 759–768.

Author's Publications

Journal Publications

[1] Zhang, Zhiping, Qing-Guo Wang and Yong Zhang. Relationship on Stabilizability of LTI Systems by P and PI Controllers. *the Canadian Journal of Chemical Engineering.* Vol. 85, No. 3, 2007.

[2] Tang, Wei, Qing-Guo Wang, Zhen Ye and Zhiping Zhang. PID Tuning for Dominant Poles and Phase Margin. *Asian Journal of Control.* Vol. 9, No. 4, 2007.

[3] Zhang, Zhiping, Yunqiu Li, Shuang-Hua Yang and Qing-Guo Wang. Load Minimization Design for Internet-based Control Systems with Dynamic Performance Specifications. *To appear in the Special Issue on Network Control, International Journal of Systems Science.*

Journal Submissions

[4] Wang, Qing-Guo, Zhiping Zhang and Karl Johan Astrom. Guaranteed Dominant Pole Placement with PID Controllers. *Submitted to Automatica.*

[5] Sun, Jitao, Qing-Guo Wang, Zhiping Zhang and Chen Xiang. New Criteria of Exponential Stability for Nonlinear Time-varying Delay Systems. *Submitted to Journal of Optimization Theory and Applications.*

Conference Publications

[6] Tang, Wei, Qing-Guo Wang, Xiang Lu and Zhiping Zhang. Why Ti=4Td in PID Tuning?. *9th International Conf. on Control, Automation, Robotics and Vision, Dec. 2006.*